Exotic mesons

L. G. Landsberg

Institute of High Energy Physics, Serpukhov
Usp. Fiz. Nauk **160**, 1–56 (March 1990)
(Extended version of an invited paper presented at the XXIV Rencontre de Moriond, at Les Arcs, Savoie, France, on 12–18 March 1989)

A review is given of the current state of searches for, and investigations of, exotic mesonic states in hadronic reactions, J/ψ decays, and γ, γ collisions. These experiments have led in recent years to the discovery of a number of mesonic states whose properties do not fit into the simple quark model of "ordinary" ($q\bar{q}$) mesons. The new particles appear to be very serious candidates for exotic hadrons. The current state of the E/iota problem and the nature of the E(1420) meson are discussed.

INTRODUCTION

Studies of the physics of resonances, which have now been continuing for more than a quarter of a century, have led to a significant change in our ideas on the nature of hadrons, i.e., strongly interacting particles. The subject went through a period of rapid development, following the classical work of Alvarez, Maglich, and others, which led to the discovery of the ω mesons. Within a relatively short period of time, several hundred new particles—baryons and mesons—were discovered. A summary of their properties can be found in a weighty special issue of Physic Letters B.[1]

It has become clear that, contrary to previously held views, none of these hadrons can be regarded as an elementary particle, and that we shall have to dig much deeper before we can conclude that the "elementary level" has been reached. Colored quarks and gluons were discovered in the course of these investigations, and quantum chromodynamics, which describes the interactions between these fundamental objects, was created. It was found that quarks were indeed the structural elements of hadronic matter, and were responsible for the diversity of the hadronic world. It has been established that all known hadrons fit into the SU(3) systematics that reflects their very simple quark structure: mesons are $q\bar{q}$ systems consisting of quark-antiquark valence pairs, whereas baryons consist of three valence quarks (qqq). Of course, these valence structures are surrounded by a virtual "sea" of quark-antiquark pairs and gluons, but it is the fundamental valence particles that determine the principal quantum numbers and the hadron systematics.

However, since the early days of the quark era, and almost up to the present time, it was not clear whether there were hadrons with more complicated valence composition, i.e., multiquark mesons ($qq\bar{q}\bar{q}$), baryons ($qqq\bar{q}\bar{q}$), and dibaryons (qqqqqq). The advent of quantum chromodynamics led to the natural assumption that gluons could also play the part of the fundamental valence structural elements, i. e., there should be mesons consisting of gluons only (they are referred to as glueballs[2]) or mixed hadrons consisting of valence quarks and gluons. The latter are the so-called hybrids or meiktons ($q\bar{q}g$ or qqqg).[3–5] All these new types of particle are usually referred as exotic hadrons.

There is a considerable number of theoretical models of exotic hadrons. It has been suggested that exotic particles consist of "readymade hadrons" and decay into colorless components without the creation of additional $q\bar{q}$ pairs from vacuum.[6] If there is no kinematic suppression, decays of this kind can have a very considerable width (these are the so-called superallowed transitions). The corresponding particles are therefore practically unobservable. According to Ref. 7, they can only appear as singularities in the P matrix. It has been shown in the approximation of a large number of degrees of freedom (the $1/N_c$ expansion) that the widths of the four-quark exotic mesons are greater than the usual width.[8]

However, it has also been suggested that there are relatively narrow exotic states within the complex internal colored structure of these objects and within the singularities of color dynamics. Thus, if an exotic hadron consists of two colored parts that are separated in space (e.g., because of the presence of a centrifugal barrier), then its decay to the final states that are color singlets will be suppressed. Such exotic particles can be characterized by normal or anomalously narrow decay widths, depending on the degree of suppression that in turn depends on the mechanism of decoloration of the decay states.[9]

There is considerable interest in searches for different types of exotic particle. It may be expected, however, that the cross sections for the production of these new objects with complex internal color structure, and the associated anomalously small widths, will be suppressed in comparison with the characteristic cross sections for hadrons with the ordinary quark composition. This has meant that searches for exotic states have been rather complex, and have remained unsuccessful for a considerable length of time. However, advances in experimental techniques achieved in recent years have resulted in a considerable change in this situation. New areas of research have developed as a result of experiments with e^+e^- colliding beams (studies of hadronic states that arise in J/ψ decays in $\gamma\gamma$ interactions). However, apparently experiments with hadron beams carried out at a qualitatively new level, using high luminosity systems capable of recording and identifying both charged and neutral secondary particles, and able to handle processes with cross sections in the nanobarn range, must be regarded as the most important development.

All this has led to significant advances in our knowledge about hadron families and to the discovery of several new particles whose properties are difficult to explain in terms of

 0038-5670/90/030169-35$01.00

the simple quark model of the structure of hadrons. These particles have become very serious candidates for exotic hadrons.

In this review, we have attempted to outline the present state of the physics of exotic hadrons with light valence u, d, and s quarks and gluons. We have made extensive use of the proceedings of the workshop on glueballs, hybrids, and exotic hadrons, ("Glueballs 88," BNL USA held between 29 August and 1 September 1988)[12] which examined the searches for exotic states and suggested further investigations. Much of our review will be concerned with problems in meson spectroscopy, since studies of exotic baryons are at an early state of their development, and the overall situation is still very uncertain.

2. TYPES OF EXOTIC HADRONS

We know that all the exotic states of hadrons can be subdivided into three groups.

2.1. Exotic states of the first kind

These are states with explicitly exotic quantum numbers such as the electric charge, strangeness, isotopic spin (mesons with $|Q|\geqslant 2$ or $|S|\geqslant 2$ or $I>1$; baryons with $|Q|>2$ or $I>3/2$ or $S>0$). Such particles simply cannot have the usual quark structure such as $q\bar{q}$ or qqq, and must necessarily be exotic multiquark states.

2.2. Exotic states of the second kind

These are particles with exotic combinations of quantum numbers such as spin J, parity P, and charge parity C, which hadrons with ordinary quark structure cannot have. For example, for neutral $(q\bar{q})$ mesons with total quark spin s and orbital angular momentum l, the parity and charge parity are known to be given by $P=-(-1)^l, C=(-1)^{l+s}$, so that such mesons can only have the following combinations of quantum numbers: $C=P=(-1)^J$ or $(-1)^{J+1}$, and also $C=(-1)^J, P=(-1)^{J+1}$. There cannot be $(q\bar{q})$ states with $C=(-1)^{J+1}$ and $P=(-1)^J$ or $J=0$ and $C=-1$ (if $J=0$ then $s=l=0$, 1, $C=+1$). The exotic sets of meson quantum numbers are therefore as follows: $J^{PC}=0^{+-},0^{--},1^{-+},2^{+-},3^{-+}$), etc. All forms of exotic mesons such as multiquark states and hybrids and glueballs[1)] can have values of J^{PC} (see the Notes at the end of this paper).

2.3. Exotic states of the third kind

These are hadronic states with latent exotic properties (the so-called cryptoexotic hadrons). They do not have external exotic features, and their complex internal structure can only be established indirectly by examining particular features of their characteristics, e.g., anomalously small widths, anomalous decay channels, special production modes, and so on. Exotic hadrons of all kinds can also belong to this class.

3. SEARCHES FOR EXOTIC STATES OF THE FIRST KIND

These searches have been in progress for a considerable time, but have not resulted in notable success. Occasional reports of the observation of such clearly exotic objects were subsequently refuted by more accurate experiments.

There are at present only two possible candidates for this category of exotic mesons.

3.1. U mesons

The U mesons constitute an isotopic quartet of particles with isospin $I=3/2$, strangeness $S=-1$, and mass ~ 3.1 GeV ($U=U^+, U^0, U^-, U^{--}$ and the corresponding antiparticles $\bar{U}\equiv\bar{U}^-,\bar{U}^0,\bar{U}^+,\bar{U}^{++}$). Possible evidence for the U mesons decaying according to the scheme $U\to\Lambda\bar{p}+$ (charged pions) was obtained in the WA-62 experiment[10] with the hyperon beam at CERN and, subsequently, in an experiment with the BIS-2 spectrometer at the Joint Institute for Nuclear Research,[11] using the neutron beam of the Serpukhov accelerator. The cross section for the production of U mesons, multiplied by the decay probability for a particular channel, was found in these experiments to be of the order of a few microbarns. Existing U-meson data must be regarded only as an indication of the possible existence of such clearly exotic particles, and they require further confirmation.

U mesons have also been looked for in $p\bar{p}$ annihilation reactions at $P_{\bar{p}}=8$ and 9 GeV/c (Refs. 12 and 13), but these searches have not been successful. However, upper limits have been established for the production cross sections, and available data on U mesons and neighboring states are summarized in Table I and in Figs. 1–4.

3.2. Mesons with isospin $I=2$ in $\gamma\gamma$ collisions

Mesons with $I=2$ may reveal themselves indirectly during the production of pairs of vector mesons in $\gamma\gamma$ collisions: $\gamma\gamma\to VV'$. The models described in Refs. 14b and 15 suggest that experimental data on the $\gamma\gamma\to\rho^0\rho^0$ and $\gamma\gamma\to\rho^+\rho^-$ reactions can be explained by interference between isoscalar and isotensor exotic mesons in intermediate states of the $\gamma\gamma\to(X)\to VV$ reaction (Table II and Fig. 5; Ref. 16).

However, these models are not unique and may not provide a rigorous description of all the data on $\gamma\gamma\to X\to VV'$ reactions for differenty types of vector mesons (cf. Fig. 5). It is therefore very important to perform direct searches for signs of such exotic resonances in other reactions, e.g., in the production of $\rho^\pm\rho^\pm$ systems in central collisions of the form $pp\to n(\rho^+\rho^+n)$, or in the antiproton annihilation process $\bar{p}n\to(\rho^-\rho^-)\pi^+$, etc. We note that certain mesonic states, e.g., $\zeta(1480)\to\rho^0\rho^0$, that may be four-quark mesons of this kind, have been observed in $\bar{p}p$ annihilation. Searches for exotic states in $\bar{p}p$ annihilation will be considered below (see Sec. 11 and Table XII).

4. SEARCHES FOR EXOTIC STATES OF THE SECOND KIND

4.1. The meson M(1405) with quantum numbers $J^{PC}=1^{-+}$

The GAMS collaboration (Institute of High Energy Physics and CERN have reported the discovery of the new meson M(1405) with $J^{PC}=1^{-+}$ (Ref. 17), which is the first example of an exotic state of the second kind. This meson was recorded in the process

$$\pi^- p\to X^0 n,\quad X^0\to\pi^0\eta \tag{1}$$

at a momentum of 100 GeV/c (3×10^4 events). The main contribution to this reaction is provided by the production of the tensor meson $A_2(1320)$. However, partial-wave analysis of data on reaction (1) reveals the presence of the reaction

$$\pi^- p\to M(1405)\,n,\ M(1405)\to\pi^0\eta \tag{2}$$

TABLE I. U mesons and closely lying states.

<table>
<tr><th>Experiment</th><th colspan="6">Basic results</th></tr>
<tr><td rowspan="3">1. WA-62 (SPS CERN) Ref. 10
$\Sigma^- + N \to U + X$,
$\quad \hookrightarrow \Lambda\bar{p} + k\pi^{\pm}$,
$P_{\Sigma^-} = 135$ GeV/c</td><td>Results, Fig. 1</td><td colspan="5">Observed signals, interpreted as U mesons of mass ~ 3.1 GeV and width $\Gamma < 24$ MeV (first paper on U mesons)</td></tr>
<tr><td>$U^+ \to \Lambda\bar{p}\pi^+\pi^+$
$U^0 \to \Lambda\bar{p}\pi^+\pi^+\pi^-$
$U^- \to \Lambda\bar{p}\pi^+\pi^-$</td><td colspan="5">Signal/background-45/50 events $\sigma(U^+)\ B = 4.8 \pm 1.4 \pm 0.8$ μb per Be nucleus
Signal/background-18/28 events $\sigma(U^0)\ B = 1.2 \pm 0.7 \pm 0.2$ μb per Be nucleus
Signal/background-62/187 events $\sigma(U^-)\ B = 3.0 \pm 1.7 \pm 0.5$ μb per Be nucleus</td></tr>
<tr><td></td><td colspan="5">Total probability that the signal is due to statistical fluctuations $\lesssim 10^{-8}$
(Notation: B is the relative probability or branching ratio)</td></tr>
<tr><td rowspan="10">2. BIS-2 (Joint Institute for Nuclear Research), 70 GeV accelerator at Institute of High Energy Physics[11]
$n + N \to U + X$,
$\quad \hookrightarrow \Lambda\bar{p} + k\pi^{\pm}$,

$n + N \to \bar{U} + X$,
$\quad \hookrightarrow \bar{\Lambda}p + k\pi^{\pm}$,

$n + N \to M_{\varphi} + X$,
$\quad \hookrightarrow \Lambda\bar{p}K^+$,
$\quad \hookrightarrow K\bar{K}p\bar{p}$;
$\langle E_n \rangle \approx 40$ GeV</td><td>Results, Figs. 2 and 3</td><td colspan="5">U and $\bar{U}$ mesons observed in seven final-state spectra with $M_U = 3050 \pm 10 \pm 30$ MeV, $\Gamma(U) < 30$ MeV. This result confirms the WA-62 data. M_{φ} mesons with hidden strangeness observed in the spectra for the first time with $M_{M_{\varphi}} = 3255 \pm 10 \pm 30$ MeV, and $\Gamma(M_{\varphi}) < 30$ MeV.</td></tr>
<tr><td>Final state</td><td>Mass interval, MeV</td><td>Number of signal/background combinations</td><td>Final state</td><td>Mass interval, MeV</td><td>Number of signal/background combinations</td></tr>
<tr><td>$U^{--} \to \Lambda\bar{p}\pi^-$</td><td>3040—3080</td><td>34/33</td><td>$M_{\varphi}^0 \to \Lambda\bar{p}K^+$</td><td>3220—3260</td><td>72/178</td></tr>
<tr><td>$U^- \to \Lambda\bar{p}\pi^+\pi^-$</td><td>3020—3080</td><td>83/159</td><td>$M_{\varphi}^0 \to \bar{\Lambda}pK^-$</td><td>3240—3280</td><td>30/50</td></tr>
<tr><td>$U^0 \to \Lambda\bar{p}\pi^+$</td><td>3020—3080</td><td>120/318</td><td>$M_{\varphi}^+ \to \Lambda\bar{p}K^+\pi^+$</td><td>3240—3280</td><td>36/55</td></tr>
<tr><td>$U^+ \to \Lambda\bar{p}\pi^+\pi^+$</td><td>3020—3060</td><td>24/45</td><td>$M_{\varphi}^+ \to \bar{\Lambda}pK^-\pi^+$</td><td>3230—3290</td><td>30/38</td></tr>
<tr><td>$\bar{U}^{++} \to \bar{\Lambda}p\pi^+$</td><td>3020—3060</td><td>37/43</td><td>$M_{\varphi}^+ \to K_S^0 p\bar{p}K^+$</td><td>3240—3300</td><td>36/48</td></tr>
<tr><td>$\bar{U}^+ \to \bar{\Lambda}p\pi^+\pi^-$</td><td>3020—3060</td><td>22/39</td><td>$M_{\varphi}^- \to \bar{\Lambda}pK^-\pi^-$</td><td>3230—3290</td><td>25/46</td></tr>
<tr><td>$\bar{U}^0 \to \Lambda\bar{p}\pi^-$</td><td>3000—3040</td><td>25/45</td><td>$M_{\varphi}^- \to \Lambda\bar{p}K^+\pi^-$</td><td>3240—3280</td><td>37/55</td></tr>
<tr><td>$\bar{U}^- \to \bar{\Lambda}p\pi^-\pi^-$</td><td>3020—3040</td><td>4/17</td><td>$M_{\varphi}^- \to K_S^0 p\bar{p}K^-$</td><td>3220—3260</td><td>36/46</td></tr>
</table>

	It is important to note that the $\bar{U}$ states are not as well defined as the U states. It may be that this is due to the asymmetry of the system which has a lower acceptance for $\bar{\Lambda}$ hyperons as compared with Λ hyperons. The M_φ meson does not show clear signs of exotic behavior. It is exists, then this is an example of exotic behavior of the third kind. For U and M_φ, the magnitude of σB amounts to a few μb/nucleon.
3. E771, MPS, Ref. 12 1) $\bar{p}p \to [\bar{U}^{++} \to p\bar{\Lambda}\pi^+] + X^-$, 2) $\bar{p}p \to [\bar{U}^{+} \to p\bar{\Lambda}\pi^+\pi^-] + X^-$, 3) $\bar{p}p \to [\bar{U}^{0} \to p\bar{\Lambda}\pi^-] + X^0$, $p_{\bar{p}} = 8$ GeV/c	Results, Fig. 4 $\bar{U}$ mesons not found. The following upper limits were established for the production cross sections: $\sigma(\bar{p}p \to \bar{U}^{++} + X^{--})\, B(\bar{U}^{++} \to p\bar{\Lambda}\pi^+) < 98$ nb, $\sigma(\bar{p}p \to \bar{U}^{0} + X^{0})\, B(\bar{U}^{0} \to p\bar{\Lambda}\pi^-) < 364$ μb (90% confidence level). Total $\bar{p}$ flux in the experiment was 3.3×10^{10}; half of the total statistics has now been processed.
4. Hybrid spectrometer at SLAC[13] $\bar{p}n \to \bar{K}^0 + X^-$, $p_{\bar{p}} = 8{,}9$ GeV/c (in liquid-deuterium bubble chamber)	The hybrid spectrometer at SLAC with the 1-m liquid-deuterium bubble chamber and hadron calorimeter was used to investigate the mass spectra of $X^- = \bar{\Lambda}n\pi^-$, $\bar{\Lambda}p\pi^-\pi^-$, $\bar{\Sigma}^-n$, $\bar{\Sigma}^\pm n\pi^\mp\pi^-$, $\bar{\Sigma}^-p\pi^-$ in the range $2{:}2 < m(X^-) < 3{:}6$ GeV. Exotic states such as U etc. were not seen in this mass range. Upper limits were found for the cross sections.

Decay state of X^-	Upper limit of σB μb, (90% confidence level)
$\bar{\Lambda}n\pi^-$	1.23
$\bar{\Sigma}^-n$	1.63
$\bar{\Lambda}p\pi^-\pi^-$	0,68
$\bar{\Sigma}^-p\pi^-$	0.50
$\bar{\Sigma}^\pm n\pi^\mp\pi^-$	0.57

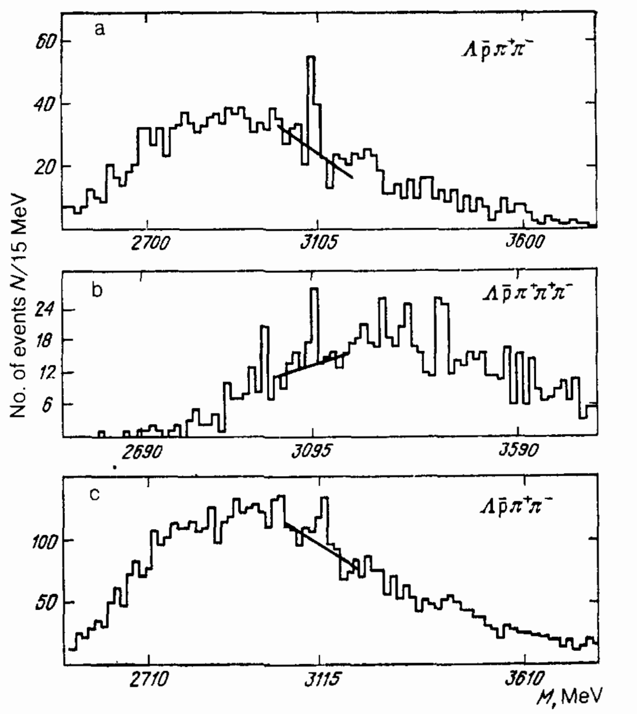

FIG. 1. The WA-62 experiment that produced the first data on U mesons in the $\Sigma^- + N \to (\Lambda\bar{p} + K\pi^\pm) + X$ reaction for $P_\Sigma = 135$ GeV/c. The figure shows the effective-mass spectrum for the states $\Lambda\bar{p}\pi^+\pi^+$ (a) $\Lambda\bar{p}\pi^+\pi^+\pi^-$ (b), and $\Lambda\bar{p}\pi^+\pi^-$ (c).

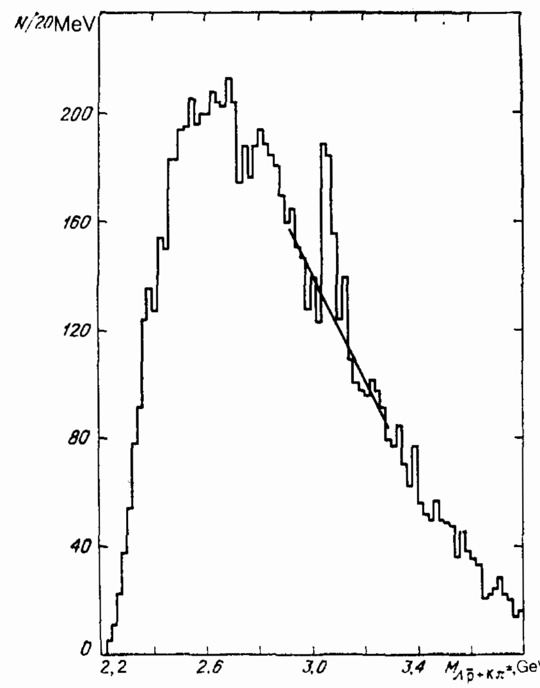

FIG. 2. The BIS-2 experiments in which a search was made for U mesons in the $n + N \to (\Lambda\bar{p} + k\pi^\pm) + X$ reactions. The total effective-mass spectrum is reproduced for the states $(\Lambda\bar{p}\pi^+)$, $(\Lambda\bar{p}\pi^+\pi^+)$, $(\Lambda\bar{p}\pi^+\pi^-)$ and $(\Lambda\bar{p}\pi^-)$.

with the cross section $\sigma(\pi^-p \to M(1405)n)B(M(1405) \to \pi^0\eta) = 9.1 \pm 2.0$ nb (Fig. 6). The meson M(1405) has the following quantum numbers: $M = 1406 \pm 20$ MeV, $\Gamma = 180 \pm 30$ MeV, $J^{PC} = 1^{-+}$, $I^G = 1^-$. It can be interpreted as the hybrid ($q\bar{q}g$) state or a multiquark meson. The same collaboration working on the Serpukhov acccelerator recorded 3×10^5 events such as (1) at 38 GeV/c. These data are being analyzed at present.

4.2. Production of mesons in the Coulomb field of the nucleus

Searches for exotic states with $J^{PC} = 1^{-+}$ have also been carried out in the Coulomb production reactions

$$\pi^+ + (Z, A) \to [\rho\pi^+, \eta\pi^+, D(1285)\pi^+] + (Z, A) \qquad (3)$$

at high primary energy ($E_{\pi^+} = 200$ GeV; experiment E272 at FNAL).[18] This method is very promising for mesons with strong enough coupling to the $\rho\pi$ channel (which is necessary for the effective Coulomb production of such particles; Fig. 7a). Searches for states with exotic quantum numbers $J^{PC} = 1^{-+}$ are continuing by means of partial-wave analysis, which becomes more reliable for the well-defined Coulomb mechanism in reaction (3).[2)]

However, a new analysis of previous measurements on the FNAL accelerator shows that the data are not sufficiently sensitive to the presence of exotic states. Only upper limits for the properties of such hadrons have been obtained (see

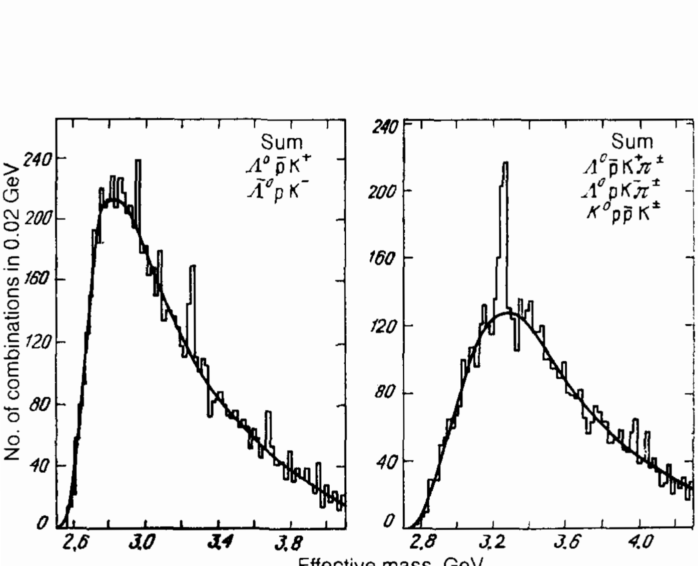

FIG. 3. The BIS-2 experiment which a search was made for mesons with hidden strangeness M_φ in the reaction

$$n + N \to M_\varphi + X, \quad M_\varphi \to \Lambda\bar{p}K^+, \quad M_\varphi \to K\bar{K}p\bar{p}.$$

The resultant effective-mass spectra are reproduced for the zero-charge states $(\Lambda\bar{p}K^+, \bar{\Lambda}pK^-)$ (a) and nonzero-charge states $(\Lambda\bar{p}K^+\pi^+, \bar{\Lambda}pK^-\pi^+, K^0_s p\bar{p}K^\pm\bar{\Lambda})$ (b).

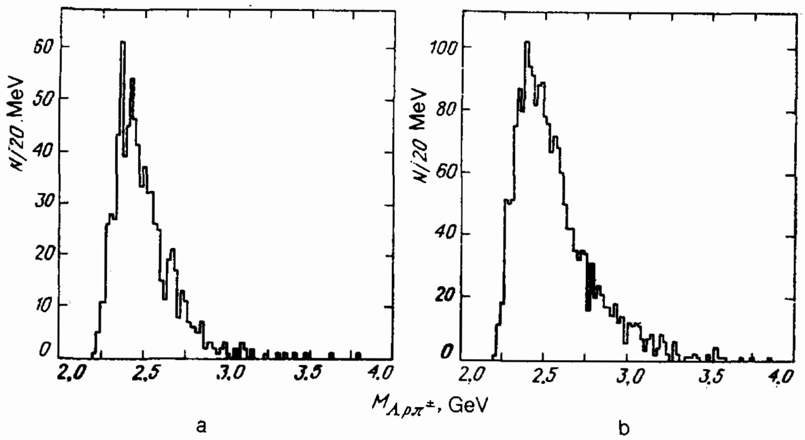

FIG. 4. Effective-mass spectra of $\bar{\Lambda}p\pi^+$ (a) and $\bar{\Lambda}p\pi^-$ (b) in the $\bar{p}p \to [\bar{\Lambda}\pi^+] + X^{--}$ and $\bar{p}p \to (\bar{\Lambda}p\pi^-) + X^0$ reactions for $P_{\bar{p}} = 8$ Gev/c (E771 BNL).

Figs. 7b–d). In particular, it has been shown that there are no exotic mesons with $J^{PC} = 1^{+-}$, mass $M < 1.5$ GeV, and decay width $\Gamma < 200$ MeV that have $B(|1^{-+}> \to \rho\pi) > 3\%$. Some evidence has also been obtained for the possible existence of a meson with $m \simeq 1.6$ GeV, which decays along the channel $\bar{\rho}(\sim 1600)^+ \to D(1285)\pi^+$; $D(1285) \to \eta\pi^+\pi^-$ with

$$\Gamma\,(\bar{\rho}\,(\sim 1600)^+ \to \pi^+\gamma)\; B\,(\bar{\rho}\,(\sim 1600)^+ \to D\,(1285)\,\pi^+) \sim 250\ \text{keV}$$

(cf. Fig. 7d). However, the quantum numbers J^{PC} have not been determined for this state because the existing statistics is not good enough. The existence of $\bar{\rho}(\sim 1660)$ requires further confirmation by more sensitive experiments.

Suggestions for new experiments on the Coulomb production of exotic mesons on the FNAL accelerator and, subsequently, on the UNK, are now under discussion.

5. SEARCHES FOR EXOTIC STATES OF THE THIRD KIND

Searches for exotic states of the third kind (crypoexotic hadrons) during the last few years have occupied a special

TABLE II. Experimental data on the $\gamma\gamma \to VV'$ reaction on the model with exotic ($qq\bar{q}\bar{q}$) mesons.

Experimental data on the $\gamma\gamma \to VV' \equiv \rho^0\rho^0, \rho^+\rho^-, \rho\omega, \omega\omega, K^{*0}\bar{K}^{*0}, K^{*+}K^{*-}, \rho\varphi, \varphi\varphi$ reaction (cf. Fig. 5)	Data obtained on the PLUTO, JADE, TASSO, ARGUS, CELLO, and TPC-2γ systems (see the reviews cited in Ref. 16 and the bibliography therein; see also the papers by G. Kernel, P. Patel, H. Bienlein, and M. Ronan at Glueballs-88, BNL, August 1988 (Refs. 93–96)

Basic results:

1. The four-quark exotic meson state[14,15] may contribute to the $\gamma\gamma \to X \to VV'$ reactions (cf. Fig. 5a)
2. The $\gamma\gamma \to \rho^0\rho^0$ reaction exhibits a sharp rise in the cross section near the threshold; $R(\rho^0\rho^0/\rho^+\rho^+) = \sigma(\gamma\gamma \to \rho^0\rho^0)/\sigma(\gamma\gamma \to \rho^+\rho^-) \gtrsim 5$ (cf. Fig. 5b). The data on $\rho\rho$ production in photon interactions are in agreement with the four-quark model of exotic mesons in the intermediate state. Interference with ($qq\bar{q}\bar{q}$) mesons having $I = 0$ and $I = 2$ explains the large ratio $R(\rho^0\rho^0/\rho^+\rho^-)$, since

$$R(\rho^0\rho^0/\rho^+\rho^-) = \left(\frac{1}{3}A_0 + \frac{2}{3}A_2\right)^2 \left[\frac{\sqrt{2}}{3}(A_0 - A_2\right]^{-2}$$

where A_2, A_0 are the amplitudes for states with $I = 2$ and 0.

3. The ($qq\bar{q}\bar{q}$) model with $J = 2^+$ gives rise to a difficulty when an attempt is made to describe the angular distribution for $\gamma\gamma \to \rho^0\rho^0$; near the threshold, the angular distribution is in better agreement with the quantum numbers of intermediate mesons, 0^+ *
4. Experimental data on $\gamma\gamma \to \rho\rho$ can also be described but in a way that does not rely on the hypothesis of exotic ($qq\bar{q}\bar{q}$) mesons.
5. The processes $\gamma\gamma \to \rho\omega$, $\omega\omega$, $K^*\bar{K}^*$ cannot be described by a single model with exotic mesons in the intermediate state; additional exchange diagrams in the t channel are necessary, at least (cf. for example, Fig. 5c).
6. The upper limits for $\sigma(\gamma\gamma \to \rho^0\varphi)$ are much lower than predicted by the model with the ($qq\bar{q}\bar{q}$) resonances (see Fig. 5d). This is a serious difficulty for this model [although it must be remembered that different ($qq\bar{q}\bar{q}$) resonances contribute to different reactions].

*)Recent data obtained on ARGUS for the $\gamma\gamma \to \rho^0\rho^0$ reaction with larger acceptance and better statistics show that the angular distributions for the $\rho^0\rho^0$ system are in good agreement with $J^P = 2^+$ (Ref. 93). These data and the ARGUS results for $\gamma\gamma \to \rho^+\rho^-$ (Ref. 94) can be regarded as evidence in support of the model and interference of ($qq\bar{q}\bar{q}$) mesons with $I = 2$ and $I = 0$ in intermediate states.

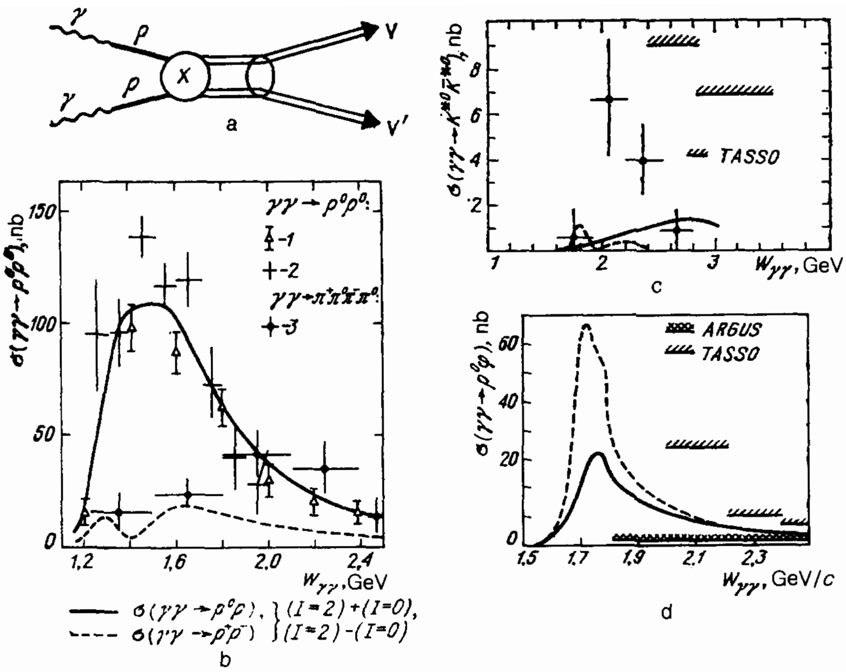

FIG. 5. Studies of the $\gamma\gamma\to VV'$ reactions: a—diagram for the process $\gamma\gamma\to(X)\to VV'$, b—the cross sections $\sigma(\gamma\gamma\to\rho^0\rho^0)$, (1—CELLO, 2—TASSO, solid curve—model with interference between intermediate exotic ($qq\bar{q}\bar{q}$) states with $I=0$ and $I=2$) and $\sigma(\gamma\gamma\to\rho^+\rho^-$; 3—JADE data on $\gamma\gamma\to\pi^+\pi^0\pi^-\pi^0$ in the mass region of ρ^+ and ρ^-, without subtracting the nonresonant background, i.e., the upper limit for $\gamma\gamma\to\rho^+\rho^-$; dashed curve-prediction of the model with ($qq\bar{q}\bar{q}$) mesons. c—Cross sections $\sigma(\gamma\gamma\to K^{*0}\bar{K}^{*0})$ obtained on ARGUS [TASSO data are the upper limits; dashed curve-prediction of the model from Ref. 14 with intermediate ($qq\bar{q}\bar{q}$) mesons, solid curve—QCD predictions in the version by Brodskiĭ *et al.*]. d—Upper limits for $\sigma(\gamma\gamma\to\rho^0\varphi)$, obtained on ARGUS and TASSO (limits obtained on TPC/2γ are practically the same as those established on ARGUS). Solid and dashed curves—predictions of the model from Ref. 14 with intermediate ($qq\bar{q}\bar{q}$) mesons for different values of the model parameters.

place in nanobarn hadron spectroscopy. Since the complex internal structure of cryptoexotic particles can only be deduced from indirect dynamic indicators, experiments performed so far have been relatively difficult to carry out. Their success has been largely due to the successful choice of exclusive processes involving hadronic systems for which qualitative considerations predict a better defined manifestation of exotic states. Some examples of this approach will be given in Secs. 5.2 and 5.3. Despite the complexity of the searches for cryptoexotic particles, it is precisely in this area

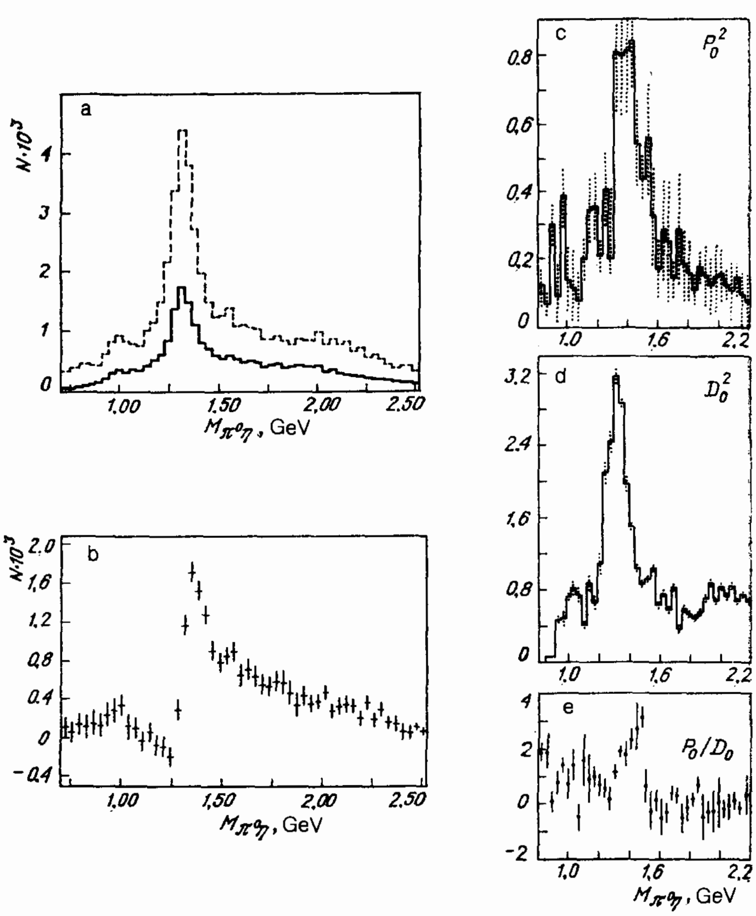

FIG. 6. Discovery of the meson $M^0(1405)\to\pi^0\eta$ with $J^{PC}=1^{-+}$ by the GAMS collaboration: a—effective-mass spectrum of $\pi^0\eta$ in the $\pi^-p\to(\pi^0\eta)n$ reaction at $P_\pi=100$ GeV/c, solid histogram—measured spectrum, dashed histogram—spectrum corrected for acceptance (top); the spectrum is dominated by the $A_2(1320)$ meson; b—forward/backward asymmetry for the $\pi^-p\to(\pi^0\eta)n$ reaction in the angle of emission of the η meson in the Gottfried-Jackson system (the asymmetry may be due to interference between the dominant D wave and the P wave; c–e—results of a partial-wave analysis of the $\pi^-p\to\pi^0\eta n$ reaction, i.e., the D and P wave intensities and the phase difference between them. The resonant character of the P wave correspond to the production of M(1405) ($J^{PC}=1^{-+}$). The phase difference is in agreement with the existence of two resonances $A_2(1320)$ and M(1405) in the D and P wave with similar mass.

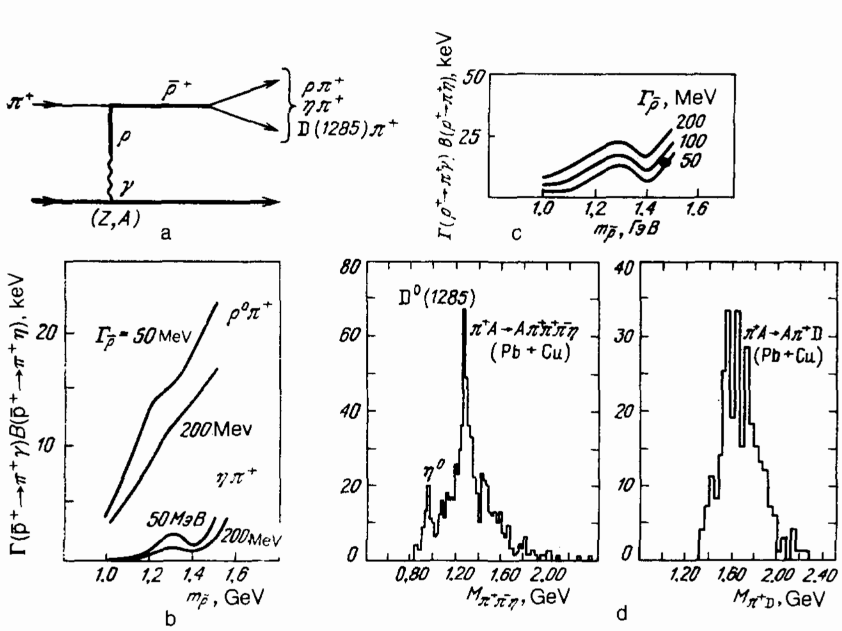

FIG. 7. An experiment (E272, FNAL) in which a search was made for ρ mesons with exotic quantum numbers $I^G = 1^-$ and $J^P = 1^-$ in the Coulomb field of the nuclei. The mesons were looked for in a partial-wave analysis of the $\pi^+ + (Z,A) \to (\rho\pi^+, n\pi^+, D(1285)\pi^+] + (Z,A)$ reaction (states with $J^PLM^\eta = 1^-Pl^+$ were selected in the investigation of the $\rho\pi^+$ and $\eta\pi^+$ systems; states with 1^-S1^+ were selected for the $D(1285)\pi^+$ system; M is the z component of spin in the Gottfried–Jackson system and η is the exchange factor for the Coulomb process, $M^\eta = 1^+$). a—Diagram for the reaction with the production of the $\bar{\rho}^+$ meson in the Coulomb field of the nucleus. b—Upper limits (at the 1σ level) for $B(\bar{\rho}^+ \to \rho\pi^+)$, obtained in the vector dominance model, using data on the Coulomb cross sections for meson widths $\Gamma = 50$ and 200 MeV in searches for the decays $\bar{\rho}^+ \to \eta\pi^+$ and $\bar{\rho}^+ \to \rho\pi^+$ (assuming that $B(\bar{\rho}^+ \to \rho\pi + \eta\pi^+ = 1)$. c—Upper limits (at the 1σ level) for $\Gamma(\bar{\rho} \to \pi^+\gamma)B(\bar{\rho}^+\eta)$ and $\Gamma_{\bar{\rho}} = 200$, 100, and 50 MeV, based on experimental data. d—Searches for $\bar{\rho}^+ \to \pi^+ D(1285)$ in the Coulomb reaction: the mass spectrum of $D(1285)\pi^+$ revealed a certain structure, but the statistics were too poor to reach any specific conclusion about the existence of the $\bar{\rho}^+$ mesons decayng along the channel containing the D(1285) meson.

that considerable advances have been made in recent years, and a few very serious candidates for exotic hadrons have emerged.

Searches for cryptoexotic states are intimately related to experiments in which more precise information is obtained about the structure of the families of ordinary mesons and baryons. Improved data are also essential for the interpretation of new resonances, since exotic particles are by definition "extra" states that do not fit into the scheme of ordinary mesonic nonets.

5.1. Table of (q$\bar{q}$) mesons

There have been considerable advances in recent years in the systematics of standard (q$\bar{q}$) mesons. This is illustrated by the new table of meson families, based on the latest experimental data (Table III). There are ambiguities at some points in this table but, on the whole, we now know (or know approximately) the structure of ten meson families. This is quite remarkable if we recall that, just a few years ago, there was only one-half of this number of families. Moreover, it is clear from the table that there is a number of "extra" hadrons that do not fit into the existing scheme. Many of these particles are serious candidates for the cryptoexotic class, and will be discussed in detail in later Sections.

5.2. Some decay channels for exotic hadrons

5.2.1. Decays of the form $M_{exp} \to M\varphi$ or $N_{exp} \to N\varphi$

The $\varphi\pi$ or $\varphi\rho$ systems that have nonzero isotopic spin [$u\bar{u}$–$d\bar{d}$) quarks] and hidden parity ($s\bar{s}$ quarks) exhibit unique properties that can be exploited in searches for multiquark mesons with hidden strangeness and hybrid mesons. The coupling between the (q$\bar{q}$) quarkonium states with $I = 1$ and the $\varphi\pi$ system is suppressed by the Okubo–Zweig–Iizuka (OZI) rule, whereas for the ($s\bar{s}$) mesons ($I = 0$) it is suppressed by isotopic invariance. This means that states that are strongly coupled to $\varphi\pi$ or $\varphi\rho$ should probably have an exotic quark structure.

We also note that isoscalar states of the form $\varphi\omega$, $\varphi\varphi$, $\varphi\eta$, $\varphi\eta'$ should have similar properties. To be more precise, we can say that in this case OZI suppression should apply to $(1/\sqrt{2})(u\bar{u} + d\bar{d}) \to \varphi\omega$, $\varphi\varphi$, $\varphi\eta$, $\varphi\eta'$ and $s\bar{s} \to \varphi\omega$ decays (here we have an analogy with $\Psi' \to \Psi\pi\pi$). However, $(s\bar{s}) \to \varphi\varphi$, $\varphi\eta$, $\varphi\eta'$ decays may be suppressed relatively weakly (because of the production of the additional $s\bar{s}$ pair from vacuum and the contribution of a large $s\bar{s}$ component of η, η' mesons).

The quantity

$$R_M = \frac{B(M \to \varphi\pi)}{B(M \to \omega\pi)}, \tag{4}$$

i.e., the ratio of the decay widths of OZI forbidden and allowed decays of ordinary (q$\bar{q}$) mesons can serve for isovector mesons as a convenient practical criterion of exotic properties. It may be expected that the ratio R_M will be quite small, e.g., $\sim 1/200$–$1/400$, for such mesons. It is indeed this situation that occurs, for example, for the B(1235) meson (the q$\bar{q}$ state $^1P_1$; see Table III) for which $R_B < 5 \times 10^{-3}$ (Ref. 20). At the same time, the magnitude of this ratio for exotic states can be quite high (~ 1). All these questions will

TABLE III.

1) The properties of $(q\bar{q})$ mesons

n	L	S_{L_J}	J^{PC}	$I=1$	$S=\pm1$	$I=0\ \left(\approx \frac{1}{\sqrt{2}}(u\bar{u}+d\bar{d})\right)$	$I=0\ (\approx s\bar{s})$
1	0	$^1S_0$	0^{-+}	π	K	η	η' (958)
1	0	$^3S_1$	1^{--}	ρ (770)	K^* (892)	ω (783)	φ (1020)
1	1	$^1P_1$	1^{+-}	B (1235)/b_1 (1235)	Q (1400)/K_1^* (1400), Mixed with 1^{++} K_1^*	H (1190)/h (1170)	h_1' (1380) ▲
1	1	$^3P_0$	0^{++}	δ (980)/a_0 (980)?	$\varkappa$ (1350)/K_0^* (1430)	ε (1300)/f_0 (1400)	f_0' (1525) ▲
1	1	$^3P_1$	1^{++}	A_1 (1270)/a_1 (1260)	Q (1280)/K_1^* (1270), Mixed with 1^{+-} K_1^*	D (1285)/f_1 (1285)	D′ (1530)/f_1' (1530) ▲
1	1	$^3P_2$	2^{++}	A_2 (1320)/a_2 (1320)	K^* (1430)/K_2^* (1430)	f (1270)/f_2 (1270)	f′ (1525)/f_2' (1525)
1	2	$^1D_2$	2^{-+}	A_3 (1680)/π_2 (1670)	L (1770)/K_2^* (1770)		
1	2	$^3D_1$	1^{--}				
1	2	$^3D_2$	2^{--}				
1	2	$^3D_3$	3^{--}	g (1690)/ρ_3 (1690)	K^* (1780)/K_3^* (1780)	ω (1670)/ω_3 (1670)	φ (1850)/φ_3 (1850)
1	3	$^3F_4$	4^{++}	a_4 (2040)	K^* (2060)/K_4^* (2075)	h (2030)/f_4 (2050)	ξ (2210)/f_4' (2210) ▲
2	0	2^1S_0	0^{-+}	π (1300)?	K (1460)	η (1280)	η (1400)
2	0	2^3S_1	1^{--}	ρ (1465)?	K^* (1415)		φ (1680)?

TABLE III (continued)

2) "Extra" mesons-possible candidates for exotic behavior	
$J^{PC}=0^{++}$	ε (900), S^*/f_0 (975) (Possibly , δ/a_0 (980)?), S_1 (991), S_2 (988), ε′ (1430), ζ/X (1480) (Possibly , 2^+?), G (1590), X (1750) (Possibly , 2^{++}?), X (1920) (Possibly , 1^{-+}, 2^{++}?)
$J^{PC}=0^{-+}$	ι (1440)/η (1430)
$J^{PC}=1^{--}$	C (1480)/ρ (1480)
$J^{PC}=1^{++}$	E (1420)/f_1 (1420) (или D′ (1530)/f_1' (1530)?)
$J^{PC}=2^{++}$	θ (1720)/f_2 (1720), X (1810), g_T (2010)/f_2 (2010), $g_{T'}$ (2300)/f_2 (2300), $g_{T''}$ (2340)/f_2 (2340)

Notes:

(1) The symbol ▲ indicates states that have recently been found in the LASS installation; their status is still not finally established.
(2) The table contains a number of features that have not been finally explained. For example, it has been suggested that the $\delta(980)/f_0(980)$ nonet is in fact a $(qq\bar{q}\bar{q})$ meson.
(3) States such as Q and L are strange mesons without definite G-parity. Such states belonging to nonets with $J^{PC}=1^{+-}$ and 1^{++} or 2^{-+} and 2^{--} will therefore mix.
(4) The list of "extra" mesons does not claim to be complete or to present the final interpretation.
(5) Some mesons in this table have not been reliably identified.

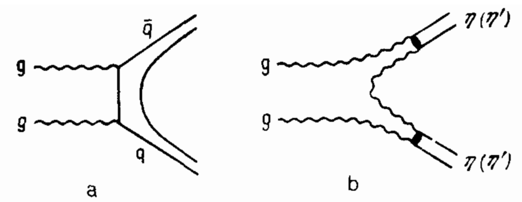

FIG. 8. Quark diagrams for glueball decays (a) and gluon decolorization (b).

be discussed in greater detail in a later Section in the context of experiments that have led to the discovery of the new vector meson $C(1480)\to\varphi\pi^0$ that is a possible exotic particles[20] (see Sec. 6).

Studies of decays involving φ mesons offer a new and promising way of searching for exotic baryons with hidden strangeness: $[N_{\exp}\equiv(\mathrm{qqqqs\bar{s}})]\to p\varphi;\Delta\varphi$. For ordinary (qqq) baryons (q = u or d), such decays are suppressed by the OZI rule. The criterion for exotic properties in this case is $R_N = B$ (baryon$\to p\varphi$, $\Delta\varphi$)$/B$(baryon$\to p\omega$, $\Delta\omega$), which is analogous to (4).

5.2.2. Gluon decoloration and decays of glueballs along the $G\to\eta\eta$, $\eta\eta'$, $\eta'\eta'$ channels

Figure 8 shows the decay schemes for glueballs in different two-meson channels with allowance for the quark diagrams [which can also be valid for ordinary ($\mathrm{q\bar{q}}$) mesons] and diagrams for glueball decoloration that are specific for glueballs.[21]

Gluon decoloration is due to the strong coupling of η and η' mesons to two-gluon states, which manifests itself in $J/\Psi\to\gamma gg\to\gamma\eta$, $\gamma\eta'$ decays. The analysis of Ref. 21 shows that glueballs can be expected to have a high probability of $G\to\eta\eta$, $\eta\eta'$, $\eta'\eta'$ decays (if the mass M_G is large enough) as compared with the $G\to\pi\pi$, KK decays. Processes involving η' mesons provide a particularly significant contribution. The characteristic hierarchy of decays (Table IV) can be predicted for glueballs in a purely qualitative way. The high probability of decay along two-particle channels involving η and η' mesons can thus serve as a characteristic indicator of a glueball.

5.2.3. $G\to 4\pi^0$ decays

Ordinary mesons such as $M = (\mathrm{q\bar{q}})$ are expected to have a very low ratio

$$\frac{B\,(M\to 4\pi^0)}{B\,(M\to 4\pi)}\sim\frac{1}{50}. \tag{5}$$

Actually, the decays of ($\mathrm{q\bar{q}}$) mesons along channels involving charged pions are sharply enhanced by ρ-meson production:

$$M\to\rho^0\rho^0\to 2\pi^+2\pi^-,\quad \rho^0\pi^+\pi^-\to 2\pi^+2\pi^-,$$
$$\rho^+\rho^-\to\pi^+\pi^-2\pi^0,\quad \rho^+\pi^-\pi^0\to\pi^+\pi^-2\pi^0.$$

At the same time, since the $\rho^0\to 2\pi^0$ decays are forbidden, this mechanism cannot enhance the $M\to 4\pi^0$ decays, which in turn lead to (5), which is in good agreement with experiment. Table V lists the ratios $4\pi^0/4\pi$ (Ref. 22) for a number of known ($\mathrm{q\bar{q}}$) mesons.

For glueballs, (5) is no longer valid because the gluon decoloration diagram cannot contribute to $G\to\rho\rho$ decays (all the verticles in Fig. 8b should typically have zero "flavors" and ρ mesons have isotopic spin $I = 1$). Moreover, the $G\to 4\pi^0$ decays should proceed via the gluon decoloration mechanism. $G\to 4\pi^\pm$ decays are thus enhanced by the production of ρ mesons (as for the ordinary mesons) and $G\to 4\pi^0$ are enhanced by the contribution of the gluon decoloration diagrams. Quantitative estimates[21] show that, for glueballs with $J = 0$,

$$\frac{B\,(G\to 4\pi^0)}{B\,(G\to 4\pi)}\sim\frac{1}{5}. \tag{6}$$

It follows that for ordinary mesons $M = (\mathrm{q\bar{q}})$, the probability of decay into the $4\pi^0$ meson is very low

$$B(M\to 4\pi^0)\sim 10^{-2}\div 10^{-3}, \tag{7}$$

whereas for glueballs we expect the much higher value

$$B(G\to 4\pi^0)\approx 10^{-1}. \tag{8}$$

5.2.4. Additional remarks on glueball decays

It has been suggested that radiative decays of glueballs ($G\to\gamma\gamma$) should be suppressed relative to the corresponding decays of ($\mathrm{q\bar{q}}$) mesons because radiative decays are due to the interaction between electromagnetic quanta and the electric charges of quark fields, and glueballs do not contain valence quarks. In particular, Chanowitz[23] used this idea to formulate a criterion for selecting glueballs from mesons in decays of the form $J(\psi)\to\gamma(gg)\to\gamma X$ enriched with the gluon component (see Sec. 5.3.1). We now introduce the stickiness parameter[23] S

$$S=\frac{\Gamma\,(J/\psi\to\gamma X)}{\mathrm{LIPS}_1}\left(\frac{\Gamma\,(X\to\gamma\gamma)}{\mathrm{LIPS}_2}\right)^{-1} \tag{9}$$

where LIPS is the Lorentz-invariant phase volume for the corresponding decay process.

The parameter S is determined, very approximately, by the ratio of the color and electric charges of the parton constituents of the hadron under investigation. Hence, for glueballs that are weakly mixed with quarks (electrically neutral colored constituents) we should have

$$S_G\gg 1,\qquad S_G\gg S_{(\mathrm{q\bar{q}})}. \tag{10}$$

However, these two glueball criteria must be used with caution, especially when S is relatively low. First, it is not at all clear to what extent the radiative decays of glueballs are sup-

TABLE IV.

$G\to P_1P_2$ decay	$\pi\pi$	$\eta\eta$	$\eta\eta'$	$\eta'\eta'$
Magnitude of the square of the matrix element	$\ll 1$	1	10	30

TABLE V.

Meson	D (1285)	f (1270)	h (2030)
$\frac{4\pi^0}{4\pi}$	$<\frac{1}{500}$	$\sim\frac{1}{30}$	$<\frac{1}{50}$

pressed by possible mixing with quark fields. Second, even ordinary $(q\bar{q})$ mesons can in some cases have an anomalously small two-photon decay width $\Gamma_{\gamma\gamma}$ (and a relatively large S), e.g., in a particular region of the singlet-octet mixing angle for mesons ($\Gamma_{\gamma\gamma}=0$ for the quark configuration[24] $(u\bar{u}+d\bar{d}-5s\bar{s})$) or because of the spatial structure of the wave function for radially-excited $q\bar{q}$ states. It will be useful in our subsequent analysis of the nature of mesons to investigate one-photon and two-photon decays $M\to M'+\gamma$ and $M\to\gamma\gamma$ at the same time.

The decay of glueballs that are neutral in quark flavors should not, in general, depend on the final state flavors. However, this conclusion may change radically when the phase volumes and the decay kinematics are taken into account. For example, the matrix element for the decay of $J=0$ glueballs should be $A(gg\to q\bar{q})_{J=0}\sim m_q$ (because of the conservation of helicity,[23] i.e., this case should be dominated by the $s\bar{s}$ decays of glueballs (this is a direct analogy with the well-known relationship for weak leptonic decays of pseudoscalar mesons $\Gamma(\pi\to\mu\nu)\gg\Gamma(\pi\to e\nu)$.

The dependence of the $g\to q\bar{q}$ transition probability on quark flavor can also be due to hadron confinement: the bound gluon acquires a constituent mass and, if this mass is $\sim 2m_Q$, the $q\to Q\bar{Q}$ transitions will be enhanced for the given quark flavor Q (Ref. 26).

5.2.5. Decays of hybrid mesons

Let us now examine the decays of hybrid mesons $|q\bar{q}g\rangle$ with the lowest masses that correspond to the S-wave states of valence quarks and gluons.[23] Decays of the hybrids $|(q\bar{q})_8^{l=0}g_{TE}\rangle$ (Table VI) can be represented by the following scheme:

$$|(q\bar{q})_8^{l=0}g_{TE}\rangle\to|(q\bar{q})_8^{l=0}(q\bar{q})_8^{l=1}\rangle$$

$$\to\left[\begin{array}{l}\text{decoloration mechanism : rearrangement}\\ \text{of quarks or soft gluon exchange}\end{array}\right]$$

$$\to|\underbrace{(q\bar{q})_1^{l=0}(qq)_1^{l=1}}_{\text{S-wave}}\rangle\to|\underbrace{q\bar{q}\rangle^{l=0}+|q\bar{q}\rangle^{l=1}}_{\text{S-wave}}, \qquad (11a)$$

$$\to\underbrace{|(q\bar{q})_1^{l=0}(q\bar{q})_1^{l=0}}_{\text{P-wave}}\rangle\to|\underbrace{q\bar{q}\rangle^{l=0}+|q\bar{q}\rangle^{l=0}}_{\text{P-wave}}; \qquad (11b)$$

where the subscripts represent the color state of the $(q\bar{q})$ system (color octet or singlet). The colored tube model[25] suggests that the decays of the lightest hybrids $|q\bar{q}g_{TE}\rangle$ are dominated by processes such as (11a), i.e., two-meson decays in which one meson is produced in the orbital ground state $^1S_0$ or $^3S_1$ and the other meson is in the orbitally excited P_1 state. It follows that hybrid meson decays $H\to\pi\rho$, $\pi\eta$ etc. may be suppressed, and the situation may be dominated by decays of the form $H\to\pi B(1235)$, $\pi D(1285)$. The colored tube model[25] has led to a number of proposals for experiments involving searches for hybrid mesons in decay channels containing B(1235) and D(1285) mesons.[3)] The masses of the hybrid mesons in this model lie above 1.9 GeV, and the expected number of hybrids with small widths is very small.

5.3. Production of exotic hadrons

We have already noted that successful searches for exotic hadrons rely on the right choice of reactions in which they are produced, for which *a priori* considerations suggest that particular mechanisms of exotic-meson production are reasonably well defined against background processes.

One of the most interesting candidates for exotic states of the third kind have been observed in the charge-transfer reactions $\pi^-p\to M^0\pi$, dominated by single-pion exchange i.e., low transferred momenta [the C(1480) meson (see Sec. 6), the G(1590) meson (see Sec. 8), and the $g_T(2010)$, $g_{T'}(2300)$, $g_{T''}(2340)$ mesons (see Sec. 7)]. One suggestion is that exotic states may be produced in diffractive processes: in some models, the pomeron can have a cryptoexotic component (up to about 20%), which gives rise to the diffractive production of exotic hadrons with cross sections up to[9] ~ 1 μb. Systematic searches for these exotic diffractive processes have not as yet been carried out. It is possible, however, that the baryon with hidden strangeness $N_\varphi(1960)$, which was observed in experiments by the BIS group at the Joint Institute for Nuclear Research, is in fact due to a similar diffractive mechanism.[27]

Searches for exotic states have also been carried out in nonperipheral type reactions, e.g., in central collisions or in experiments with higher transferred momenta, namely, $|t'|\sim 0.3-0.4$ (GeV/c^2) (Sec. 8).

TABLE VI. Quantum numbers of hybrid mesons $|q\bar{q}g\rangle$ with the lowest mass that correspond to S states of quarks and gluons.

Type of valence gluon	Quantum numbers of the $(q\bar{q})$	
	$^1S_0$, $J^{PC}=0^{-+}$	$^3S_1$, $J^{PC}=1^{--}$
Transverse electric valence gluons: g_{TE}, $J^{PC}=1^{+-}$	$J^{PC}=1^{--}$, $(^1S_0)\,g_{TE}$	$J^{PC}=0^{-+}, 1^{-+}, 2^{-+}$, $(^3S_1)\,g_{TE}$
Transverse magnetic valence gluons: g_{TM}, $J^{PC}=1^{--}$	$J^{PC}=1^{+-}$, $(^1S_0)\,g_{TM}$	$J^{PC}=0^{++}, 1^{++}, 2^{++}$, $(^3S_1)\,g_{TM}$

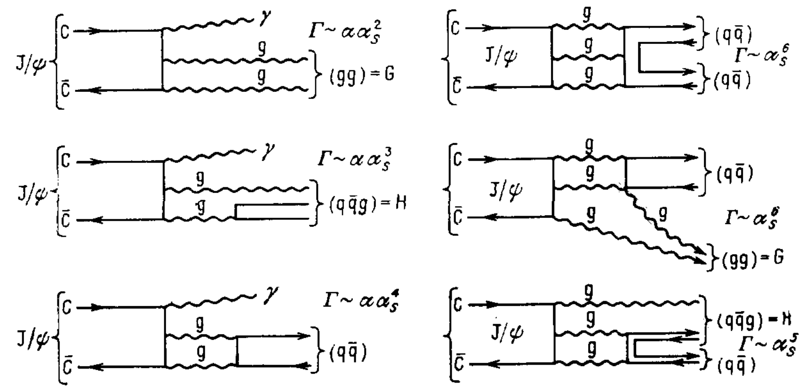

FIG. 9. Diagram for radiative and two-meson decays of J/ψ particles [cf. (13) and (14)].

Different mechanisms of glueball production have been examined for a number of processes in which particularly favorable conditions are expected for searches of exotic objects. It is even possible that glueball production will be the dominant feature of such processes.

5.3.1. Radiative decays of J/ψ particles

Radiative decays of the form

$$J/\psi\to\gamma(gg)\to\gamma X \qquad (12)$$

have long been regarded as very promising from the point of view of searches for glueballs and, possibly, hybrid states as well. Simple estimates made in the lowest-order QCD approximation have shown[23] that the probability of radiative J/ψ decays with the production of glueballs G, hybrids H, and $(q\bar{q})$ mesons take the form (Fig. 9)

$$\Gamma(J/\psi\to\gamma G)\sim O(\alpha\alpha_s^2),$$
$$\Gamma(J/\psi\to\gamma H)\sim O(\alpha\alpha_s^3),$$
$$\Gamma(J/\psi\to\gamma|q\bar{q}\rangle)\sim O(\alpha\alpha_s^4).$$

Hence, the predicted hierarchy of decay widths is

$$\Gamma(J/\psi\to\gamma G)>\Gamma(J/\psi\to\gamma H)>\Gamma(J/\psi\to\gamma|q\bar{q}\rangle). \qquad (13)$$

When the J/ψ particle decays into two mesons, and the process is dominated by three-gluon intermediate states, similar estimates show that

$$\Gamma(J/\psi\to H|q\bar{q}\rangle)\sim O(\alpha_s^5),$$
$$\Gamma(J/\psi\to G|q\bar{q}\rangle)\sim O(\alpha_s^6),$$
$$\Gamma(J/\psi\to|q\bar{q}\rangle|q\bar{q}\rangle)\sim O(\alpha_s^6),$$

or

$$\Gamma(J/\psi\to H|qq\rangle)>\Gamma(J/\psi\to G|q\bar{q}\rangle)\sim\Gamma(J/\psi\to|q\bar{q}\rangle|q\bar{q}\rangle), \qquad (14)$$

i.e., processes with the formation of hybrids are particularly prominent.

It is important to note that perturbative estimates for the widths of exclusive decay channels of J/ψ mesons [see (13) and (14)] are very approximate because they do not take into account the effects of interaction in the final state.

Experiments on J/ψ decays and, above all, those on the decays indicated in (12), are known to play an important part in searches for glueballs, (the data on $\iota(1440)$ and $\theta(1720)$ mesons were obtained by analyzing this process (cf. Sec. 9). Apart from the above physical properties of (12), this is also due to a number of its experimental advantages. First, the resonant production of J/ψ mesons in e^+e^- collisions has a large cross section and low background. This has meant that existing e^+e^- storage rings such as SPEAR and DCI, working in the region of the J/ψ resonance energy, have produced statistics corresponding to the production of about 10^7 J/ψ particles. Second, the decay process (12) has a relatively high probability $(B(J/\psi\to\gamma\gamma(gg))=6\pm2\%$, and can be satisfactorily investigated. Finally, there are very high luminosity systems that can readily select exclusive channels in the decay of the J/ψ particles (Mark III and DM2). We note that the most recently commissioned e^+e^- collider BEPC (PRC), which has high luminosity and produces very monochromatic beams, will be used in the near future to improve the statistics of J/ψ decays by more than an order of magnitude. A further improvement will become possible when the high-current e^+e^- factories or the SUPERLEAR antiproton source will become available (the resonance reactions $\bar{p}p\to J/\psi\to X$ and $\bar{p}p\to\chi\to X$ can take place in antiproton beams).

5.3.2. Glueballs and central production processes

At high primary energies, collisions between sea gluons (in hadronic interactions) can lead to the efficient production of gluons in these gg collisions (Fig. 10a). It is possible that these processes are in fact responsible for the rise in the total cross section with energy.[29] Gluon-gluon interactions become increasingly important as the primary energy increases. This is clear, for example, from the preferential production of gluon jets in the Sp̄pS collider.

Favorable conditions for glueball searches can be established by the gg collision mechanism in exclusive neutral production reactions $(x(M_0)_F\sim 0)$ at high primary energies:

$$h+N\to h_f(M^0)N_s, \quad M^0\to P_1P_2, \qquad (15)$$

which are dominated by two-pomeron exchange [see the diagram of Fig. 10b] where h_f and N_s represent the fast (f) and slow (s) particles in the laboratory frame. According to QCD, pomeron exchange can be interpreted as a multigluon process. The specific kinematics of reaction (15) is conven-

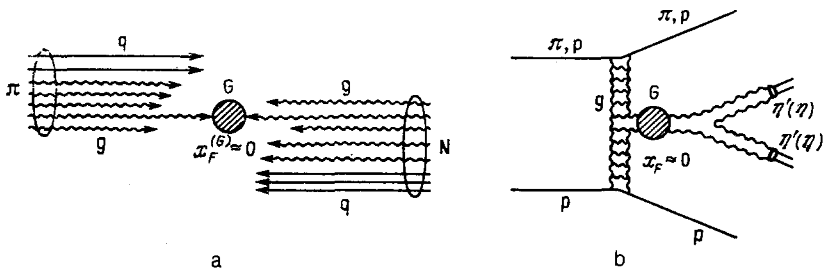

FIG. 10. a—Central production of particles in collisions between "sea" gluons in hadronic interactions at high energy, b—double pomeron exchange (multigluon process) in central production reactions.

ient for the detection of gluon production and decay (see Ref. 30 for further details).

5.3.3. Exotic mesons and some hadron reactions

Processes in which the production of ordinary particles is strongly suppressed by the OZI selection rule offer interesting possibilities for searches for exotic hadrons. On the other hand, the OZI rule may be violated during the production of exotic states because of their complex internal color structure. This facilitates the separation of processes with cryptoexotic particles.

As an example, consider the reaction

$$\pi^- p \to \varphi\varphi n, \tag{16}$$

which, in the case of the nonresonant production of the $\varphi\varphi$ system, should be suppressed by the OZI selection rule as compared with the process

$$\pi^- p \to \varphi K^+ K^- n, \tag{17}$$

that is allowed by this rule (see the diagrams of Fig. 11a). However, experimental data[31] show that the OZI rule is strongly violated in reaction (16). This can be explained by a resonance effect in the intermediate gg channel (see Fig. 11a) that leads to the formation of glueballs (or hybrids).

The nonresonant reaction $\pi^- p \to \varphi\pi^0 n$ should also be suppressed by the OZI rule (cf. Fig. 11c). However, if we have the cascade production and decay of an exotic state M_{exo} in the reaction $\pi^- p \to M_{exo} n$, $M_{exo} \to \varphi\pi^0$, the OZI rule may be appreciably violated because of the complex valence quark or the quark-gluon composition of M_{exo}. This is accompanied by an increase in the cross section for the corresponding process. The partial violation of the OZI rule is due to a reduction in the number of hard gluons in the intermediate state during the formation of M_{exo} (cf. diagrams of Figs. 11c and d).

Studies of OZI-forbidden reactions may thus turn out to be a promising way of searching for exotic hadronic states, since the production of cryptoexotic particles in such processes may be less highly suppressed than the production of hadrons with the usual quark structure. Of course, the reverse situation obtains in the majority of other processes in which ordinary mesons are well represented in reactions, whereas the mechanisms responsible for the production of cryptoexotic states provide a very small contribution. As in illustration, consider reactions of the form

$$K^- p \to M^0 Y. \tag{18}$$

We know that glueballs and hybrids (the coupling of gluons to quarks is flavor independent) and ordinary mesons with hidden strangeness ($s\bar{s}$) have a high probability of decay with the emission of KK pairs. However, whereas $s\bar{s}$ mesons are produced in (18) with high cross sections, these processes are not particularly appreciable for exotic states, and do not have high probabilities. Data on (18) can therefore be used to elucidate the nature of different mesonic states. Such studies have reinforced arguments in support of the interpre-

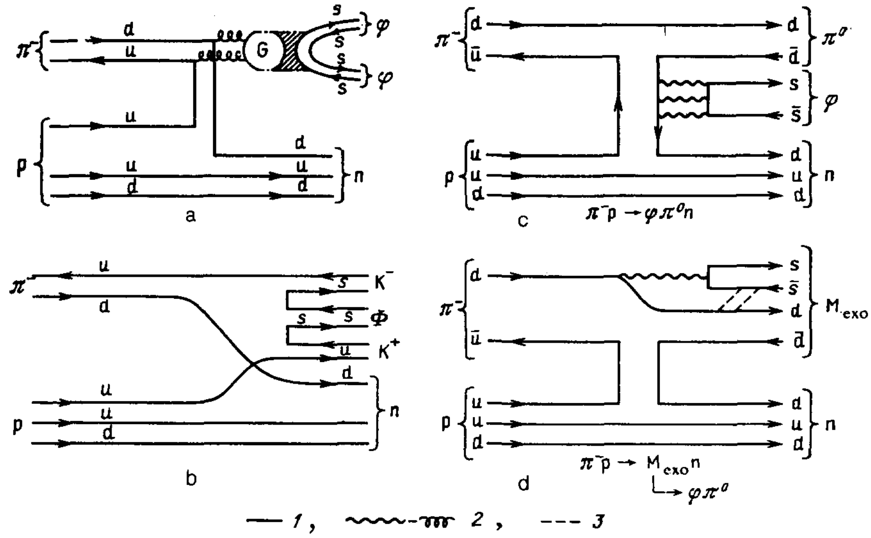

FIG. 11. a, b—Diagrams for the $\pi^- p \to \varphi\varphi n$ reaction (16), suppressed by the OZI selection rule, and for the allowed reaction $R_g = B(g(1680) \to \varphi\pi^0)/B(g(1680) \to \omega\pi^0)$ (17). c, d—Diagrams for the nonresonang reaction $J^P LM^\eta = 1^- Pl^+$, suppressed by the OZI rule, and for the cascade process $\pi^- p \to \varphi K^+ K^- n$ in which there is partial OZI suppression. Notation: 1—quark, 2—hard gluons, 3—soft gluons.

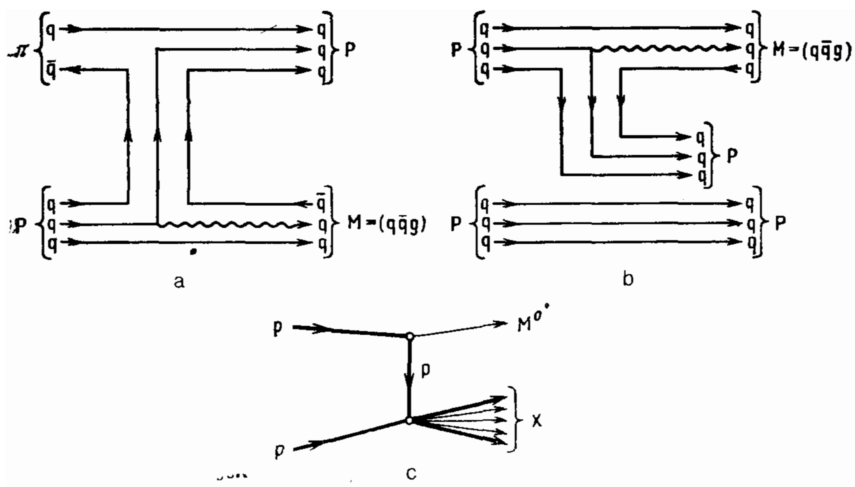

FIG. 12. a—Production of a hybrid meson in a process with baryon exchange in πN interactions. b—Production of a hybrid meson in a process with baryon exchange in pN interactions. c—Process with baryon exchange of the quasiexclusive type (inclusive in the lower vertex).

tation of the $\theta(1710)$ meson as a glueball (cf. Sec. 9) and, conversely, have led to the conclusion that the $\xi(2220)$ meson is more likely to be a $s\bar{s}$ state with spin 4.

5.3.4. Exotic states and baryon exchange processes

Studies of resonance states have often led to the suggestion that the excitation of the internal color degrees of freedom, accompanied by the formation of exotic quark or quark-gluon systems, should occur more effectively in processes with high momentum transfers and, in particular, in reactions such as back scattering due to baryon exchange (see, for example, Refs. 32 and 33). It is expected that the creation of exotic states in such processes can be characterized by cross sections that are comparable with the cross section for the production of ordinary pairs. As an example of this type of back scattering reaction, Fig. 12a shows the diagram for the production of a hybrid meson in the process $\pi^- p \to n_f M^0$ (cf. Ref. 3).

Several experiments have now been carried out in which a search was made for exotic mesonic states in baryon exchange reactions:

$$\pi^+ p \to \Lambda_f S^{++}, \tag{19}$$

$$\pi^- n \to p_f X^{--}, \tag{20}$$

$$\pi^- p \to (p_f \pi^-)(\bar{p} p_s). \tag{21}$$

Upper limits have been found for the cross sections for these processes, and some of them are listed in Table VII (Refs. 36–39).

Data have also been obtained on the back scattering of a number of known mesonic states and on the elastic back scatter of $\pi^\pm$ and charge transfer with baryon exchange ($\pi^- p \to n_f \pi^0$). These data lead to the following conclusions: (1) for a given energy, the cross sections for all the two-particle and quasi-two-particle processes with baryon exchange are not very different from one another and (2) at $E_\pi \sim 12$ GeV, these cross sections lie in the range 0.3–0.7 μb and decrease with energy in accordance with the expression $\sim p_{\text{lab}}^{(2-2.7)}$; at lower energies, this variation is much more rapid $\sim p_{\text{lab}}^{(5-7)}$.

Extensive researches for the production of mesons generally, and exotic mesons in particular, in the back scattering of pions be nucleons are impeded by experimental difficulties. The point is that the mesons are emitted in these processes in backward directions in the center of mass system (cf. Fig. 12a), so that, in the laboratory frame, the decay products have a soft momentum spectrum and a wide angular distribution. The detection efficiency for these mesons in experiments performed with magnetic spectrometers is usually low. There are also difficulties with the identification of the decay products of mesonic resonances.

All these difficulties can be obviated by investigating the production of mesonic resonances in baryon exchange processes in a proton beam, using reactions of the form

$$pp \to M^0 + (pp), \tag{22}$$

$$\to M^+ + (pn), \tag{23}$$

$$\to M^+ + d \tag{24}$$

(cf. Fig. 12b).

The mesons produced in these reactions are emitted in the forward direction, and can be relatively readily recorded in a large-aperture magnetic spectrometer. The charged particles that emerge from these decays can be identified by a set of gas-filled Cherenkov counters. A strong trigger signal can be generated and then amplified whenever two slow protons appear in the special system surrounding the liquid-hydrogen target [for (22)]. When reactions such as (22)–(24) are recorded, the experiments have to carried out at proton energies that are not too high (~ 20 GeV) because the cross sections for exclusive processes with baryon exchange fall rapidly with increasing primary energy.

The cross sections for (22)–(24) can be normalized to the data on the two reactions

$$pp \to d\pi^+, \tag{25}$$

$$pp \to d\rho^+, \tag{26}$$

which also involve baryon exchange. The corresponding cross sections were measured in a precision magnetic spectrometer at CERN for primary momentum $p_p = 21.1$ GeV/c, and amount to $\sigma(pp \to d\pi^+) = 15.1 \pm 1.5$ nb, and $\sigma(pp \to d\rho^+) = 15.9 \pm 2.4$ respectively.[34] The cross sections for the processes $pp \to dA_2$ (A_1), which were also observed in this experiment, have similar magnitudes. Since the "stickiness" between p and n as they produce a deuteron gives rise

TABLE VII. Searches for mesons with clearly exotic properties in processes with baryon exchange.

Reference	Reaction	Method	Results
[36]	$\pi^+p \to \Lambda_f^0 S^{++}$, (19) $p_{\pi^+} = 9{,}8$ GeV/c	MPS, BNL spectrometer: 1) missing-mass spectrum for S^{++} 2) reconstruction of the reactions $\pi^+p \to \Lambda_f^0(K^+\pi^+)$, (19a) $\to \Lambda_f^0(p\bar{\Sigma}^+)$, (19b) $\to \bar{n}\pi^+$ (Λ_f etc. is a particle emitted in the forward direction).	The following upper limits were obtained for the cross sections of the reactions: $\sigma(19) < 20$ nb, $\sigma(19a) < 10$ nb for $M_{S^{++}} < 2$ GeV
[37]	$\pi^+p \to \Lambda_f^0 S^{++}$, (19) $p_{\pi^+} = 12$ GeV/c	Ω-spectrometer at CERN Missing-mass spectrum for S^{++} (for all events and for events with multiplicity ⩽2)	The following upper limits were obtained for the cross sections GeV $\sigma(19) < 60$ nb ($1 < M_{S^{++}} < 2{,}65$ GeV), $\sigma(19) < 150$ nb ($2{,}65 < M_{S^{++}} < 3{,}6$ GeV)
[38]	$\pi^-d \to p_f X^{--} p_s$, $\to p_f X^- n_s$, $p_{\pi^-} = 13{,}2$ GeV/c	Streamer chamber at SLAC Searches for X^{--} and X^- formed in processes with baryon exchange $X^{--} = \pi^-\pi^-$, $\pi^-\pi^-\pi^-\pi^+$, $4\pi^-2\pi^+$, $p\bar{p}\pi^-\pi^-$, $X^- = \pi^-\pi^-\pi^-$, $3\pi^-2\pi^+$, $p\bar{p}\pi^-$ (exposure sensitivity 240 events/μb	No statistically significant maxima were found in X^{--} and X^- in the mas range 1.8–3.2 GeV with cross sections comparable with the cross section for reverse production of ρ(770 amount to ~0.25 μb
[39]	$\pi^-d \to (p_f\pi^-)(\bar{p}p_s)$, $p_{\pi^-} = 16$ GeV/c The production of mesons in the $p\bar{p}$ system in the lower vertex (baryon exchange reaction) was investigated	MPS, BNL spectrometer. 7000 examples of this reaction were recorded. No peaks with $\Gamma < 30$ MeV were found for the $p\bar{p}$ system in the mass range 1900–2400 MeV	For the states X(2020) and X(2200) previously observed in the CERN experiments with the Ω-spectrometer, the upper limit was found to be $\sigma < 2$–3 nb (at the level of two standard deviations). These data are in conflict with the results obtained with the Ω-spectrometer

to a reduction in the cross section by more than an order of magnitude and the reduction may well be by a factor of the order of 100 (cf. Ref. 35), the expected cross sections for reactions (22) and (23) may be quite high (~0.2–1 μb). This offers interesting possibilities for searches for exotic mesons in this type of process. The energy dependence of the cross sections for (25) at high energies is relatively difficult to establish because the only data available on this reaction correspond to $p_p < 5$ GeV/c, i.e., the region in which the cross sections decrease rapidly (the reduction is slower in the region $p_p \sim 10-12$ GeV for reactions with baryon exchange). All that can be said at present is that, for high energies, the cross section is described by $\sigma(pp \to d\pi^+) \sim p_{lab}^{(2.5-4)}$. Similar behavior may be expected in the case of the cross sections for (22)–(24).

Nevertheless, searches for exotic mesonic states in processes with baryon exchange can also be made at higher proton energies (this is often of considerable interest because it is a means of better identification of seconary particles and mesons under investigation). In inclusive processes with baryon exchange in the lower vertex (cf. Fig. 12c)

$$p + N \to M + X_{l.\,vertex}, \tag{27}$$

the cross sections are very slowly varying functions of the primary energy E_p when all the possible states are summed for the dibaryon system. At high enough energy E_p, the secondary particles from the lower and upper vertices in Fig. 12c will be well separated in rapidity, i.e., the inclusive nature of the reaction in the lower vertex will not produce an undesirable combinatorial background when meson resonances in the upper vertex are investigated (we shall refer to these processes as quasi-exclusive). For reactions such as (27), the expected cross sections are of the order of a few hundred nanobarn. Searches for exotic mesons in quasi-exclusive processes such as (27) are very promising in this case.

Analysis of the deuteron spectrum from pp interactions[34] has shown that the nonresonant background near the end of this spectrum, which corresponds to the quasi-exclusive reactions $p + p \to d + X_{l.\,vertex}$, does in fact exceed by more than an order of magnitude the contribution due to the resonance processes (25) and (26), and probably confirms that quasi-exclusive reactions with baryon exchange (27) can in fact be used in searches for exotic resonances.

However, before we proceed to the extensive program of such searches, we must verify that the above conclusions about the magnitude of cross sections for the quasi-exclusive processes and their weak energy dependence are valid. This can be done quite readily for the simpler charge transfer reactions with baryon exchange

$$\mathrm{P}+\mathrm{N}\to(\pi^0)_{\text{forward}}+X_{\text{l.vertex}},\quad (\pi^0)\to 2\gamma \tag{28a}$$

$$\mathrm{P}+\mathrm{N}\to(\eta)_{\text{forward}}+X_{\text{l.vertex}},\quad (\eta)\to 2\gamma \tag{28b}$$

$$\mathrm{P}+\mathrm{N}\to(\omega)_{\text{forward}}+X_{\text{l.vertex}},\quad (\omega)\to\pi^0\gamma\to 3\gamma \tag{28c}$$

and the reaction

$$\mathrm{p}+\mathrm{N}\to(\pi^-)_{\text{forward}}+X_{\text{l.vertex}} \tag{29}$$

(in which Δ^{++} exchange is isolated).

For processes (28a)–(28c), we can readily generate a trigger at the level of about 10^{-5} (charge transfer with the release of a large amount of energy in the electromagnetic calorimeter). Studies of this type are now in progress on the SFINKS system in the 70-GeV proton beam of the accelerator at the Institute of High Energy Physics.

It is thus clear that searches for cryptoexotic hadrons can be based on different exclusive and quasi-exclusive reactions with a clear signature in which the production and decay of exotic particles is detected with a sufficient degree of confidence, as indicated by the above discussion. The situation is summarized in Tables VIII and IX. We now turn to the analysis of particular physical experiments.

6. THE VECTOR MESON C(1480) AS A POSSIBLE EXOTIC STATE

6.1. Observation of the C(1480) meson[20]

The Lepton-F system at the Institute of High Energy Physics has been used to investigate the charge transfer reaction

$$\pi^-\mathrm{p}\to(\mathrm{K}^+\mathrm{K}^-\pi^0)\mathrm{n} \tag{30}$$

at momentum $p_{\pi^-}=32.5$ GeV/c. The Lepton-F system is a combination of a large-aperture magnetic spectrometer incorporating proportional chambers and a hodoscopic 200-channel γ-spectrometer capable of efficient recording of charged hadrons and photons in the final state. The primary and secondary charged particles are identified by a system of gas-filled threshold Cherenkov counters.

TABLE VIII. Some decay channels for exotic mesons.

1. $M\to\varphi\pi$	$(q\bar q)_{I=1}\nrightarrow\varphi\pi$ (OZI forbidden)	for $M_{exo}\equiv(q\bar q s\bar s)$, $(q\bar q g)$
$\to\varphi\rho$	$(s\bar s)_{I=0}\nrightarrow\varphi\pi$ (isospin forbidden)	$R=\Gamma(M_{exo}\to\varphi\pi^0)/\Gamma(M_{exo}\to\omega\pi^0)\sim 1$
$M'\to\varphi\omega$	$(q\bar q)_{I=0}\nrightarrow\varphi\omega$ (OZI forbidden)	for $(q\bar q)$ $R\sim 1/400\div 1/200$

2. $G\to\eta\eta$, $\eta\eta'$, $\eta'\eta'$ — Typical decays for glueballs

Diagrams for glueball decays:

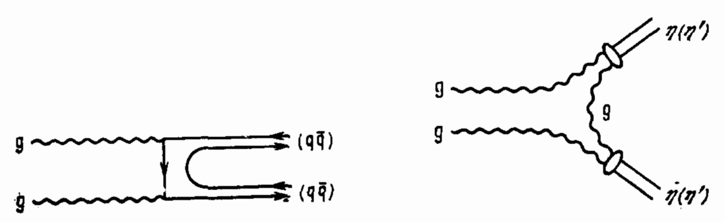

1) quark diagram (the same as for $q\bar q$ mesons) 2) gluon decolorization diagram (typical for glueballs)

Gluon decolorization mechanism due to the strong coupling between the (gg) system and the η and η' mesons. The $J/\psi\to\gamma(gg)\to\gamma\eta$, $\gamma\eta'$ decay data for glueballs with $J^{PC}=0^{++}$ were used to predict high probabilities for the $G\to\eta\eta$, $\eta\eta'$, $\eta'\eta'$ decays

The ratios of the squares of the matrix elements $|A|^2$ for the $G\to P_1P_2$ (P is the pseudoscalar meson):

$G\to P_1P_2$	$\pi\pi$	$\eta\eta$	$\eta\eta'$	$\eta'\eta'$
$\lvert A\rvert^2$	$\leqslant 1$	1	10	30

3. $M\to 4\pi^0$:

The $(q\bar q)\to 4\pi^\pm$ decay is enhanced by the ρ-meson production process $(q\bar q)\to\rho^0\rho^0\to\pi^+\pi^-\pi^+\pi^-$ etc. Hence, $B(q\bar q\to 4\pi^0)/B(q\bar q\to 4\pi)\sim 1/50$ ($\rho^0\to\pi^0\pi^0$ is forbidden).

For glueballs $G\to 4\pi^\pm$ is enhanced by the production of ρ (quark diagrams), $G\to 4\pi^0$ is enhanced by the mechanism of gluon decolorization.

The result is $B(G\to 4\pi^0)\sim 10^{-1}$,
$B(q\bar q)\to 4\pi^0)\sim 10^{-2}-10^{-3}$.

The high $G\to 4\pi^0$ decay probability is a typical property of a glueball.[22]

4. Decays of hybrid mesons in the colored tube model (cf. Ref. 25)	Decays of the lowest-mass hybrid states occur mostly along the channel with orbitally excited mesons: $\lvert q\bar q g\rangle\to\lvert S_{0;1}\rangle+\lvert P_1\rangle = \pi B(1235)$, $=\pi D(1285)$, $=\ldots\ldots\ldots\ldots$

TABLE IX. Production of exotic mesons.

1. $J/\psi \to \gamma(gg) \to \gamma G$. This decay channel is enriched with gluons and is promising from the standpoint of searches for glueballs and, possibly, hybrids.

$\Gamma(J/\psi \to \gamma G$: large glueball width

$\Gamma(G \to \gamma\gamma)$: small glueball width

$$\text{Stickiness } S_X = \frac{\Gamma(J/\psi \to \gamma X)}{\text{LIPS}_1}\left(\frac{\Gamma(X \to \gamma\gamma)}{\text{LIPS}_2}\right)^{-1}.$$

This quantity is very approximately determined by the ratio of the color to electric charges of the parton constituents of X (LIPS = Lorentz-invariant phase volume).

Glueballs: $S_G \gg 1$ and $S_G \gg S_{(q\bar{q})}$ (Ref. 23)

2. Glueballs are produced in gg collisions in central production processes of the form $h + N \to h_f (G \to P_1P_2)N_x$. The contribution of gg collisions in the central region increases with increasing $s^{1/2}$, and the glueball production may become better defined.[29,30]

3. Reactions suppressed by the OZI rule for standard ($q\bar{q}$) mesons (for example, $\pi^-p \to (\varphi\varphi)n$, $\pi^-p \to (\varphi\pi^0)n$) may be successfully used in searches for exotic mesons, i.e., cascade processes $\pi^-p \to M_{exo}n$, $M_{exo} \to \varphi\varphi$ or $\to \varphi\pi^0$. Because of the complex color structure of exotic mesons, the OZI selection mode may be strongly violated when these mesons are produced.[30,31,32,36]

4. Candidates for exotic mesons have been found in exclusive charge transfer reactions (especially processes with one-pion exchange). In some cases, the background due to peripheral processes in exclusive reactions was suppressed by using the selection criterion $|t|$)0.2 – 0.4 (GeV/c)^2.

5. There have been discussions of the possible production of exotic quark-gluon systems in particular processes involving the excitation of internal color degrees of freedom in collisions with high transferred momenta, e.g., in baryon exchange reactions or in diffraction phenomena (because of the possible exotic component of the pomeron)

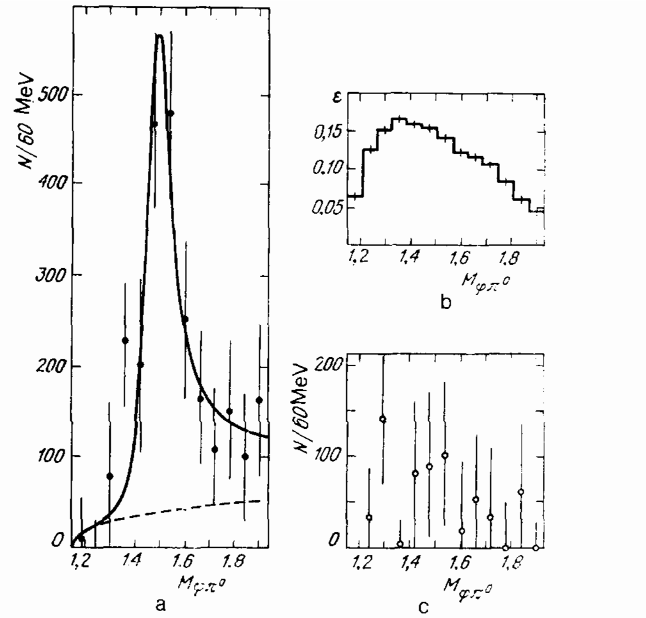

FIG. 13. a—Effective-mass spectrum of the $\varphi\pi^0$ system in the $\pi^-p \to (\varphi\pi^0)n$ reaction, weighted for the acceptance of the system. The spectrum was approximated by the relativistic Breit–Wigner formula for orbital angular momentum L = 1 and a polynomial background. The experimental resolution for $M_{\varphi\pi^0} \sim 1{,}5$ GeV was 45 MeV (FWHM). b—Acceptance of the spectrometer for the detection of the $\varphi\pi^0$ system in reaction (31). c—"Background experiment-- for the spectrum of spurious "φ"π^0 events. The mass interval used to simulate these spurious φ mesons was chosen to be $1044 < M_{K^+K^-} < 1052$ MeV. The "background" mass intervals $M_{K^+K^-}$ were selected to lie around the "φ" intervals 1030–1038 and 1058–1066 MeV ($M_{\varphi\pi^0}$ is shown along the ordinate axes in GeV.

The effective mass spectrum of the K^+K^- system in (30) has been found to have a well-defined peak corresponding to the production of the φ meson in the charge-exchange reaction

$$\pi^-p \to (\varphi\pi^0)n. \tag{31}$$

Events with φ mesons were selected from the region of the peak ($1016 < M_{K^+K^-} < 1024$ MeV). All the distribution for the $\varphi\pi^0$ system were obtained by two independent methods of subtracting the background under the φ-meson peak. In one of them, the background was determined by an integral technique, using the half-sum of events in two mass intervals adjacent to the peak (1002–1010 and 1030–1038 MeV). In the other, more sophisticated technique, the background was subtracted by subdividing the distribution under investigation into bins of values of the corresponding variable [for example, the effective mass of the $K^+K^-\pi^0$ system in (30)], and the number of events (31) in each bin was found by a fit to the φ-meson signal in the mass spectrum of the K^+K system. The two methods of subtracting the background gave very similar results, and the entire procedure used to analyze the experimental data was very stable with respect to extensive variations of the selection criteria, bin width, parameters of the φ peak, and so on. The total number of events (31) was in the range 350–400, depending on the selection criteria. It is clear from Sec. 5.2.1 and 5.3.3 that although reaction (31) is suppressed by the OZI rule for the $\varphi\pi^0$ resonant state, it is very convenient in searches for exotic mesons in the $\varphi\pi^0$ system.

The mass spectrum of the $\varphi\pi^0$ system in (31) is dominated by a peak with the following mass and width (Fig. 13a):

$$M_C = 1480 \pm 40 \text{ Mev}, \quad \Gamma_C = 130 \pm 60 \text{ Mev} \tag{32}$$

The spectrum is weighted in accordance with the acceptance of the system (Fig. 13b). The results obtained in a special "background experiment," show that the background unrelated to the φ mesons is small in this mass spectrum (Fig. 13c). The observed peak is referred to as the C-state.

The cross section for the production of the C-state has been found to be

$$\sigma(\pi^-p \to Cn)B(C \to \varphi\pi^0) = 40 \pm 15 \text{ nb}. \tag{33}$$

The uncertainties indicated in (32) and (33) include both statistical and systematic contributions.

Additional investigations have established that the peak observed in the mass spectrum of the $\varphi\pi^0$ system can not be explained by threshold effects of the deck type and is

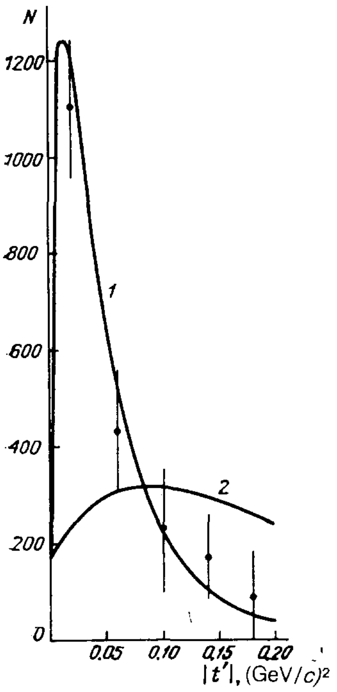

FIG. 14. Distribution of events from the C peak with the square of transferred four-momentum t', weighted for the acceptance of the system. Curve 1—fit of the experimental data by the t' dependence expected for pion exchange in (34), 2—fit obtained on the assumption of A_2 exchange in (34).

due to a new resonance—the C(1480)-meson. The contribution of the deck-effect to the cross section (33) does not exceed a few nb.

The distribution of events corresponding to the reaction

$$\pi^-p \to C(1480)n \qquad (34)$$

over the square of the transferred four-momentum $t' = t - t_{\min}$. has been investigated. The experimental data (Fig. 14) are satisfactorily described by the dependence for pion exchange. Attempts to describe t-distribution in (34) on the assumption of exchange of some other adjacent pole (A_2) were found to be unsatisfactory (the confidence level of the corresponding fit was less than 10^{-5}; cf. Fig. 14).

The dominant mechanism in the charge-transfer reaction (34) with the formation of the state C(1480) is pion exchange, which limits the possible quantum numbers of the C(1480) meson to $P = C = (-1)^J$. The $C \to \varphi\pi^0$ decay scheme shows that this state has isospin $I = 1$ and negative charge parity. This means that odd values of the total angular momentum, i.e., $J^{PC} = 1^{--}$:3^{--} etc., are the only possible ones. We can therefore probably confine our attention to the first two sets of quantum numbers, since all known mesons with $J \geqslant 3$ have masses in excess of 2 GeV.

Direct data on the quantum numbers of C(1480) can be obtained by analyzing cascade decays in the reaction

$$\begin{aligned} \pi^-P \to\ & C(1480)\,n, \\ & \hookrightarrow \varphi\pi^0, \\ & \quad \hookrightarrow K^+K^-. \end{aligned} \qquad (35)$$

The Gottfried–Jackson system [i.e., the rest system of the C(1480)] is used to analyze the $C \to \varphi\pi^0$ decay, whereas the process $\varphi \to K^+K^-$ is analyzed in the rest frame of the φ meson. The polar and azimuthal angles in these two systems are denoted by ϑ', φ' and ϑ'', φ'', respectively.

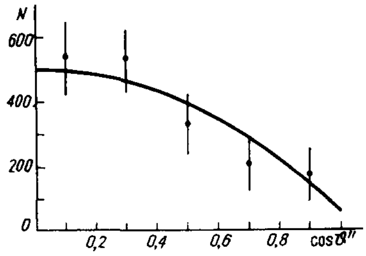

FIG. 15. Distribution of events from the C peak with $\cos\vartheta''$ in the rest frame of the φ meson, weighted for the acceptance of the system. Solid curve shows the fit obtained for these points by using the expression $dN/d\cos\vartheta''| \sim 1 - (b/3) + b\cos^2\vartheta''$; $b = -1{,}36 \pm 0.37$; θ'' is the angle between K^- and π^0 in the rest frame of the φ meson.

The distribution of events over the angle θ'' between the K^- meson and the neutral pion in the rest frame of the φ meson determines the helicity of the φ meson: for $\lambda_\varphi = \pm 1$ it should be ϑ', φ' and ϑ'', φ'', whereas for $\lambda_\varphi = 0$ it should be $dN/d\cos\vartheta'' = \text{const}\cdot\cos^2\vartheta''$. The experimental θ'' distribution was described by $dN/d|\cos\vartheta''| = \text{const}\cdot[1 - (b/3) + b\cos^2\vartheta'']$ where $b = -1.36 \pm 0.37$ (Fig. 15). This means that the helicity of the φ meson is compatible with $\lambda_\varphi = \pm 1$ (for which $b = -1.5$) and, in particular, it reliably excludes the zero spin of C(1480) for which $\lambda_\varphi = 0$, i.e., $b = 3$. The conclusion that the C-state has nonzero spin follow from the shape of the distribution $dN/d|\cos\vartheta''|$ and is independent of the assumption that one-pion exchange is the dominant process in (34). The distribution of events in the azimuthal angle θ'' between the direction of emission of K^- and the plane of the $C \to \varphi\pi^0$ decay is $dN/d\varphi'' = \text{const}\cdot\sin^2\varphi''$.

We now turn to the complete analysis of angular distributions in the cascade decays of C and φ mesons. They can be predicted for different hypothesis about the quantum numbers of the C(1480) state under particular assumptions about the mechanism responsible for reaction (34) and its density matrix $\rho_{mm'}$. The well known helicity formalism is used in this procedure. In the simplest model of one-pion exchange, the density matrix $\rho_{mm'}$ has the form $\rho_{00} = 1$, $\rho_{mm'} = 0$ for $m,m' \neq 0$. The angular distributions of the decay particles are then described by[40]

$$W(\vartheta', \varphi'; \vartheta'', \varphi'') = \text{const}\cdot\sin^2\vartheta''\cdot\sin^2\varphi''(d^J_{10}(\cos\vartheta'))^2. \qquad (36)$$

It follows that, in the rest frame of the φ meson, the distributions of the decay K-mesons in ϑ'' and φ'' (37) are in agreement with experimental data and confirm the dominance of the pion-exchange mechanism in the production of C(1480), which was established by studying the corresponding t-distribution (see Fig. 14).

If reaction (34) is domianted by pion exchange, then the quantum numbers of the C(1480) mesons should be $J^{PC} = 1^{--}$ or 3^{--}. To choose between them, we must investigate the distribution of the decay products in the process $C(1480) \to \varphi\pi^0$ over the polar angle θ' at which the neutral pion is emitted in the Gottfried–Jackson system for (34). According to (34), the angular distribution assumes one of the following two forms, depending on the possible spin values:

$$\frac{dN}{d\cos\vartheta'} = \text{const}\cdot(d^1_{10}(\cos\vartheta'))^2 = \text{const}\cdot\sin^2\vartheta' \quad (J = 1) \qquad (37)$$

or

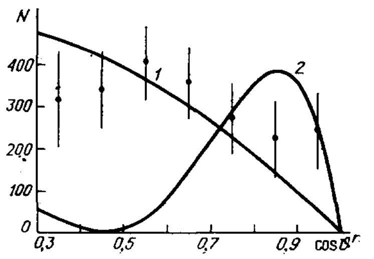

FIG. 16. Distribution of weighted events from the C peak with $\cos\theta'$ in the Gottfried–Jackson system. Curve 1—expected distribution for $J^{PC} = 1^{--}$ (37), 2—$J^{PC} = 3^{--}$ (38).

$$\frac{dN}{d\cos\vartheta'} = \text{const}\cdot(d^{12}_{10}(\cos\vartheta'))^2$$
$$= \text{const}\cdot\sin^2\vartheta'\cdot(5\cos^2\vartheta' - 1)^2 \quad (J = 3). \qquad (38)$$

The distribution of the $C\to\varphi\pi^0$ decays over the polar angle θ' is shown in Fig. 16 and takes into account the acceptance of the spectrometer which limits the effective range of angles to $0.3 < \cos\vartheta' < 1$.

It is clear from Fig. 16 that the angular distribution is consistent with the following quantum numbers of the C(1480) meson; $J^{PC} = 1^{--}$, i.e., with (37), and excludes $J^{PC} = 3^{--}$ [cf. (38)]. The corresponding confidence levels are 0.2 and 10^{-7}. For higher spin values, $J^{PC} = 5^{--}$ etc., the confidence levels for the description of the experimental angular distribution in $\cos\theta'$ are even lower than for $J^{PC} = 3^{--}$.

Analysis of the angular distributions from the $C\to\varphi\pi^0$ and $\varphi\to K^+K^-$ decays in (34) has therefore been used in a model-independent way to exclude $J = 0$ as a possible spin of C(1480) and to show that $J^{PC} = 1^{--}$ in the one-pion exchange model (OPE) for the reaction (34). This conclusion is stable and does not change when the one-pion exchange model is altered by including absorption effects.[20,40]

The quark structure of the C(1480) meson can be characterized by the very important decay probability ratio $R_c = B(C(1480)\to\varphi\pi^0)/B(C(1480)\to\omega\pi^0)$ (4), i.e., the ratio for processes that are respectively OZI forbidden and allowed for mesons consisting of u and t quarks. The authors of Ref. 20 determined R_c by using, in addition to (31), the data on the reaction

$$\pi^- p \to \omega\pi^0 n, \qquad (39)$$

obtained at momentum $P_{\pi^-} = 38$ GeV/c in experiments with the GAMS-2000 spectrometer.[41] The mass spectrum of $\omega\pi^0$ in (39) was found to contain peaks due to $B(1235)\to\omega\pi^0$ and $g(1680)\to\omega\pi^0$ decays, but statistically significant structures were not found in the region of 1.5 GeV. This defined the following lower limit:

$$R_C > 0.5 (95\% \text{ confidence level}). \qquad (40)$$

The anomalous character of this result for the C(1480) meson becomes very clear if we compare it with the data on the analogous decays of the well-known "ordinary" meson B(1235) $J^{PC} = 1^{+-}$, $(q\bar{q})$ system in the $^1P_1$ state]:

$$R_B = \frac{B(B(1235)\to\varphi\pi^0)}{B(B(1235)\to\omega\pi^0)} < 5\cdot10^{-3}. \qquad (41)$$

The upper limit for R_B in (41) was obtained by comparing the effective mass spectrum of $V\pi^0$ in reaction (31) (Lepton-F) and reaction (39) (GAMS-2000) in the region of the mass of the B(1235) meson.[20] The ratio R_B was thus found to be lower than R_c by at least two orders of magnitude. Preliminary analysis has shown that the ratio $R_g = B(g(1680)\to\varphi\pi^0)/B(g(1680)\to\omega\pi^0)$ is also very small for the G(1680) meson that is the $(q\bar{q})$ system in $^1D_3$ state.

6.2. Nature of the C(1480) meson[19,20,42–51]

There are, at least in principle, three possibilities as far as the interpretation of the data on the vector meson C(1480) is concerned. They are:

(1) The C(1480) meson has the ordinary quark structure of a meson with isotopic spin $I = 1$:

$$|C(1480)\rangle = \left|\frac{1}{\sqrt{2}}(u\bar{u} - d\bar{d})\right\rangle.$$

The rare decay $C(1480)\to\varphi\pi^0$ is highly OZI suppressed and proceeds with very low probability (less than 1% or even $\ll 1\%$). It was observed in this experiment.

(2) The C(1480) meson is the isotopically scalar meson φ' with quark composition $|C\rangle_{I=0} = |s\bar{s}\rangle$ and, since $\varphi\pi^0$ has isospin $I = 1$, the $C(1480)\to\varphi\pi^0$ decay is due to the violation of the isotopic invariance.

(3) The C(1480) meson is an exotic state, i.e., a multiquark or hybrid meson. This type of hadron can be strongly coupled to the $\varphi\pi$ system.[19]

The first possibility (rare decay of the ordinary $(1/\sqrt{2})$ $(u\bar{u} - d\bar{d})$ meson) was investigated, for example, in Ref. 43 and cannot explain the considerable departure from the OZI rule in C(1480) decays ($R_c > 0.5$ which is higher by two orders of magnitude than the corresponding ratio for other mesonic decays and hadronic reactions). It was shown in Ref. 42 that there is no secure experimental basis for this type of model at present, so that this possibility is somewhat unlikely. These questions are also discussed in Refs. 50 and 51.

The interpretation of experimental data on the C(1480) meson in terms of the ordinary $s\bar{s}$ state model decaying along the $|C\rangle_{I=0}\to\varphi\pi^0$ channel with isospin nonconservation is found to be totally excluded:[42] this model leads to a cross section of less than 0.1 nb in (33), which differs from the experimental result by three orders of magnitude.

A consistent explanation of all the properties of the C(1480) meson and, above all, the high value of R_c [cf. (40)] can be achieved by interpreting it as a cryptoexotic four-quark state with the following structure:

$$|C(1480)\rangle = \left|\frac{1}{\sqrt{2}}(u\bar{u} - d\bar{d})\, s\bar{s}\right\rangle. \qquad (42)$$

This provides a natural explanation of the isotopic spin of this state ($I = 1$) and its strong coupling to the $\varphi\pi$ system. Possible searches for four-quark vector states in the $\varphi\pi$ system were first discussed in Ref. 19. The existence of the resonant $\varphi\pi$ state was predicted on the basis of phenomenological considerations in Ref. 44.

Another possible explanation of the nature of the C meson is based on the model of hybrid states (meiktons). In this scheme (see Table VI)

$$|C(1480)\rangle = \left|\frac{1}{\sqrt{2}}(u\bar{u} - d\bar{d})\, g_{TE}\right\rangle \qquad (43)$$

where the $C\to\varphi\pi^0$ decay occurs in accordance with (11b).

The vector meikton was discussed in Ref. 4 and its mass was predicted to be about 1.6 GeV. The relative decay probability of vector meiktons along the $\varphi\pi^0$ and $\omega\pi^0$ channels should be of the same order because the coupling constant between the gluon and a pair of $q\bar{q}$ quarks is independent of their flavor.

Unless there is some new explanation of the considerable departure from the OZI rule in the decay of the C(1480) meson ($R_c > 0.5$), the hadron should therefore have an exotic structure.

Further information on the exotic structure of the C(1480) meson can be obtained by analyzing different decay channels, and also by searching for other objects of similar character. For example, Ref. 45 predicts the existence of the isoscalar partner of the C-meson, namely, $|\bar{C}\rangle = |(1\sqrt{2})(u\bar{u} + d\bar{d})s\bar{s}\rangle$, which has approximately the same mass and width as the C(1480). It is expected that the $|\bar{C}\rangle$ state will appear as a resonance in the mass spectrum of the $\omega\eta$ system. It is important to note that the analogous isoscalar state $|\bar{C}\rangle = |(1\sqrt{2})(u\bar{u} + d\bar{d})g\rangle$ can appear in the hybrid model for the C(1480) meson.

The nature of the C(1480) meson is also discussed in Ref. 46 in which processes responsible for its formation and decay are examined together with the mixing of quark combinations in the wave function of the four-quark exotic state. It is suggested that there should be exotic mesons with very similar properties, which are G and C parity conjugates. According to this hypothesis, there should be in addition to the C(1480) meson with $J^{PC} = 1^{--}$, another meson with similar mass and exotic quantum numbers $J^{PC} = 1^{-+}$. Just such a particle M(1405) with mass $m = 1406 \pm 20$ MeV and width $\Gamma = 180 \pm 30$ MeV was discovered in a totally different experiment, i.e., in the partial-wave analysis of the mass spectrum of the $\eta\pi^0$ system in the $\pi^- p \to n\pi^0$ reaction investigated in the GAMS system[17] (see Sec. 4.1). The possible coupling between these states is a question of considerable interest that requires further investigation. In particular, a different model is discussed in Ref. 47 in which the mesons C(1480) and M(1405) are G and C conjugate hybrid states (meiktons). Some other questions relating to the exotic nature of the C(1480) are discussed in Refs. 48–51.

The existence of a resonance in the $\varphi\pi$ system in the mass range under investigation is confirmed by data obtained with the Sigma spectrometer[52] in which an analysis of the inclusive process $\pi^- p \to \varphi\pi^- X$, $\varphi \to \mu^+\mu^-$ revealed a peak in the effective mass spectrum of $\varphi\pi^-$ with parameters close to those of the C(1480) meson.[53] Experiments on the photoproduction process $\gamma p \to \varphi\pi^0 p$ with $20 < E_\gamma < 70$ GeV (using the Ω-spectrometer at CERN) have also revealed a certain excess of events in the mass spectrum of the $\varphi\pi^0$ system in the region of the C(1480) meson. There are suggestions that the resonance X(1660) may be present in the $\omega\eta$ system in the $\gamma\pi \to \omega\eta p$ reaction with mass $m = 1.61 \pm 0.04$ GeV and width $\Gamma = 0.23 \pm 0.08$ GeV) ($J^{PC} = 1^{--}$ or 1^{+-} or 2^{--}).[54] The origin of this peak and its possible identification with the predicted isoscalar exotic C remain an open question.

6.3. Further investigations of the C(1480) meson

A number of new experimental studies of the properties of the C(1480) mesons, including searches for the charged partners $C(1480)^\pm \to \varphi\pi^\pm$ are being discussed at present. These experiments will be performed at the IHEP and at BNL (see, for example, Ref. 55). There is considerable interest in further studies of the C(1480) mesons in electromagnetic processes and $\bar{p}p$ annihilation.

7. g^T-MESONS AS POSSIBLE GLUEBALLS WITH $J^{PC} = 2^{++}$

Evidence for the existence of the g_T mesons was obtained by analyzing the $\pi^- p \to \varphi\varphi n$ reaction (16) (see Sec. 5.3.3.). The corresponding experiments were performed by the BNL/CCNY group using the MPS installation with a primary momentum $p_{\pi^-} = 22$ GeV/c (Refs. 31 and 56). A

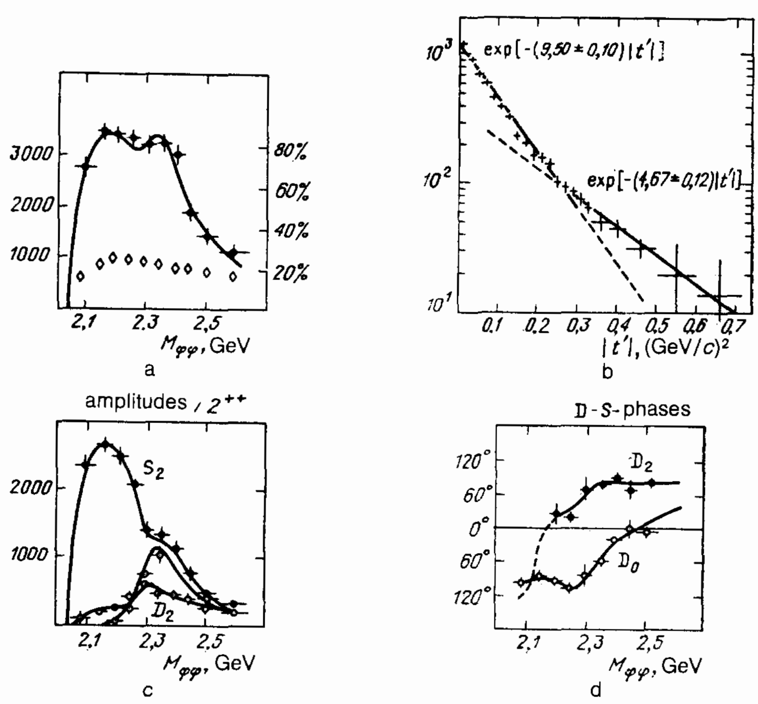

FIG. 17. The $\pi^- p \to \varphi\varphi n$ reaction (16) and data on $g_T(2010)$, $g_{T'}(2300)$, and $g_{T''}(2340)$ mesons: a—effective-mass spectrum of the $\varphi\varphi$ system (N/50 MeV) in reaction (16), weighted for the acceptance of the system; the acceptance is indicated by the symbol ◇. b The t-distribution for reaction (16). The OPE mechanism is the dominant one for small t. c, d—Partial-wave analysis of reaction (16): intensity (c) and phase difference relative to the S-wave (d) for three $J^{PC} = 2^{++}\Lambda$ waves. The curves represent a fit to the experimental points by the Breit–Wigner resonances with the parameters listed in Table VIII.

total of 6658 events of the form of (16) was recorded. Figure 17a shows the effective mass spectrum of the $\varphi\varphi$ system produced in reaction (16) and characterized by the quantum numbers $I^G = 0^+$, $C = +1$. A detailed partial-wave analysis of this reaction with allowance for the cascade decays

$$\begin{array}{l}\pi^- p \to Xn, \\ \quad \hookrightarrow \varphi \qquad\qquad + \varphi, \\ \qquad \hookrightarrow K^+K^-, \quad \hookrightarrow K^+K^-. \end{array} \tag{44}$$

has been carried out. Although it was based on the usual isobaric model, some of the features of this process have ensured that this analysis was unique. Thus, first, the two narrow states (φ-mesons) into which the mesonic system X decays make the analysis model-independent. Second, the additional information gleaned from the $\varphi \to K^+K^-$ decays can be used to obtain a unique solution when 114 partial waves are taken into account [all states with $J \leqslant 6$, $S \leqslant 2$, $L \leqslant 4$, $|M| \leqslant 6$, $P = \pm 1$, $\eta = \pm 1$, where J is the total spin of the X, S is the total spin of the two φ mesons, M is the component of J_z and the z axis of the Gottfried-Jackson system for reaction (16), P is the final-state parity, and η is the exchange parameter]. The form of the t-distribution for reaction (16) (cf. Fig. 17b) shows that it is dominated by one-pion exchange for $|t'| < 0.3$ $(\text{GeV}/c)^2$ in which case $M^\eta = 0^-$. Partial-wave analysis has shown that the $\varphi\varphi$ spectrum of Fig. 17a is almost completely saturated by the three states $J^PSLM^\eta = 2^+2SO^-(S2)$, 2^+2DO^- $(D2)$, and 2^+ODO^- $(D0)$ (Fig. 17c). The relative phases of the two D waves relative to the S wave are shown in Fig. 17d. The curves of Figs. 17c and d correspond to the description of the results of the phase analysis by three Breit–Wigner resonances g_T, $g_{T'}$, and $g_{T''}$ with $J^{PC} = 2^{++}$ and the parameters listed in Table X. The solution obtained in this way is unique: a change in even one wave is excluded at the 13σ level and an attempt to describe the system by two resonant states is excluded at the 18σ level.[56] The analysis of reaction (16) was performed in parallel with the analysis of the process $\pi^- p \to \varphi K^+K^- n$ (17) that proceeds without violation of the OZI rule. It is noticeable that the background due to process (17) in (16) is small ($\approx 13\%$) and is mostly of nonresonant character. There is a strong violation of the OZI rule in reaction (16), which can be treated as evidence for the interpretation of g_T, $g_{T'}$, and $g_{T''}$ mesons as glueballs. This interpretation has frequently been criticized (cf. the discussion in, for example, Ref. 27, which give the bibliography, and also Ref. 31). Some confirmation of the results reported by the BNL/CCNY group was provided by the WA-67 experiments on the Ω-spectrometer at CERN[58] in which the inclusive process $\pi^-\text{Be} \to \varphi\varphi + X(P_{\pi^-} = 85\ \text{GeV}/c)$ was investigated. The mass spectrum of the $\varphi\varphi$ system was found in Ref. 58 to contain a structure with maxima at $M_1 = 2231 \pm 10$ MeV, $\Gamma_1 = 133 \pm 50$ MeV and $M_2 = 2392 \pm 10$ MeV, $\Gamma_2 = 198 \pm 50$ MeV that are compatible with the $g_{T'}$ (2300) and $g_{T''}$ (2340) mesons [g_T (2010) was suppressed in this experiment by the acceptance of the system].

In view of the interpretation of the g_T mesons as glueballs, the question arises as to why they are not seen in the $J/\psi \to \gamma gg$ decays, as defined by (12), in which mesons with an enriched glueball component are naturally formed. (see Sec. 5.3.1). Moreover, the analysis of $J/\psi \to \gamma\varphi\varphi$ decays in the mass spectrum of the $\varphi\varphi$ system shows that they are dominated by states with $J^{PC} = 0^{-+}$. Lindenbaum[56] suggested in his last paper that this does not amount to any contradiction because calculations[59] indicate that the expected total probability that all the glueball g_T states will appear in the decay (12) is very low and lies below the experimental limit:

$$R_{\varphi\varphi}(g_T)_{\text{theor}} = \sum_{g_T} B(J/\psi \to g_T + \gamma)\, B(g_T \to \varphi\varphi) \approx 0{,}7 \cdot 10^{-6}, \tag{45}$$

$$R_{\varphi\varphi}(g_T)_{\text{exp}} < 8.6 \cdot 10^{-5} (90\% \text{ confidence level}). \tag{46}$$

(This is based on the MARK III data reported in Ref. 56). However, the question of observability or otherwise of the g_T mesons in J/ψ decays (12) continues to be discussed because experiments with the DM2 system[60] have established an upper limit for the other possible g_T-meson decay, namely,

$$R_{\rho^0\rho^0}(g_T) = \sum_{g_T} B(J/\psi \to \gamma g_T)\, B(g_T \to \rho^0\rho^0) < 9 \cdot 10^{-5} \quad (90\% \text{ confidence level}). \tag{47}$$

The expected value for this quantity is[59]

$$R_{\rho^0\rho^0}(g_T)_{\text{theor}} \approx 3.2 \cdot 10^{-4}, \tag{48}$$

which is in clear conflict with (47).

Other interpretations of the g_T mesons have also been discussed, e.g., as hybrids or $ss\bar{s}\bar{s}$ states.[61]

The BNL/CCNY group intend to investigate reaction (16) for large t' for which the exchange mechanism in the t-channel is different (as can be seen from Fig. 17b) and may be due to the A poles. It is possible that new mesonic states $X \to \varphi\varphi$ will appear in this region with exotic quantum numbers J^{PC} (Refs. 55 and 56). Actually, the quantum numbers of the $X \to \varphi\varphi$ in the case of pion exchange can be $J^{PC} = 0^{++}, 2^{++}, 4^{++}$, and so on. The A_I exchange mechanism allows for the possible formation of states $X \to \varphi\varphi$ with $J^{PC} = 1^{-+}$. In these experiments, the cross section for reaction (16) will be increased by reducing the primary momentum to 8 GeV/c. It is also intended to perform further investigation of the $\varphi\varphi$ system in the $\bar{p}p \to \varphi\varphi\pi^0$ and $K^-p \to \varphi\varphi\Lambda/\Sigma^0$ reactions.[55]

TABLE X. The properties of g_T mesons.[31,56]

State	Mass, GeV	Width, GeV	S2, %	D2, %	D0, %	Percentage of all $\varphi\varphi$
g_T (2010)	$2{,}011^{+0{,}062}_{-0{,}076}$	$0{,}202^{+0{,}067}_{-0{,}082}$	98^{+1}_{-3}	0^{+1}	2^{+2}_{-1}	45
$g_{T'}$ (2300)	$2{,}297 \pm 0.028$	$0.149 \pm 0{,}041$	6^{+15}_{-5}	25^{+18}_{-14}	69^{+16}_{-27}	20
$g_{T''}$ (2340)	$2{,}339 \pm 0.055$	$0{,}319^{+0{,}081}_{-0{,}069}$	37 ± 19	4^{+12}_{-4}	59^{+21}_{-19}	35

TABLE XI. New mesons: candidates for exotic states of the second kind with $I^G = 0^+$ observed by the GAMS collaboration.

Meson	J^{PC}	M, MeV	Γ, MeV	Decays	Reactions and cross sections	Results
G (1590) [22, 62, 63]	0^{++}	1587 ± 16	287 ± 50	The following decays were observed: $G(1590) \to \eta\eta,\ \eta\eta',\ 4\pi^0$, $B(G \to 4\pi) \approx 0{,}5 \pm 0{,}1$, $B(G \to \eta\eta') \approx 0{,}35 \pm 0{,}10$, $B(G \to \eta\eta) \approx 0{,}12 \pm 0{,}03$, $B(G \to K\bar{K}) < 0{,}05$, $B(G \to \pi\pi) < 0{,}05$	The charge transfer reaction (49) with predominant pion exchange $\sigma(\pi^- p \to Gn)$ $B(G \to \eta\eta) = 33 \pm 8$ nb (38 GeV/c) $= 3.8 \pm 0.7$ nb (100 GeV/c (cf. Fig. 18) Central production reaction (50) with $p_\pi = 300$ GeV/c $\sigma(\pi^- p \to p_f G(1590) p_s) \approx 0.2 \pm 0.1$ mb (for $0 < x_F < 0.3$) (Fig. 20a)	G(1590) is a strong candidate for a scalar glueball since: 1) There is a self-consistent picture of the ratios B for the main decay channels that is in agreement with the theoretical expectations for a glueball (cf. Fig. 21). 2) The G(1590) meson is well defined in the central production reaction (15) $p_\pi = 300$ GeV/c in which processes due to the gg interactions should be well defined
X (1810) [22, 64]	2^{++}	1806 ± 10	190 ± 20	The following decay was observed: $X(1810) \to 4\pi^0$. $\dfrac{B(X(1810) \to 4\pi^0)}{B(X(1810) \to \eta\eta)} = 0{,}8 \pm 0{,}3$ $\dfrac{B(X(1810) \to 2\pi^0)}{B(X(1810) \to 4\pi^0)} < \dfrac{1}{5}$	Charge transfer reaction (49) (cf. Fig. 19) $\sigma(\pi^- p \to Xn)$ $B(X \to 4\pi^0) = 8 \pm 2$ nb (100 GeV/c). Central production reaction (50) (cf. Fig. 20b) $\sigma(\pi^- p \to \pi_f^{-\prime} X(1810) p_s \times B(X \to 4\pi^0) = 40 \pm 15$ nb ($0 < x_F < 0.4$) or $\sigma(\pi^- p \to f X(1810) p_s \gtrsim 0.2$ nb ($0 < X_F < 0.4$)	X(1810) is a candidate for a tensor glueball since: (1) for ordinary ($q\bar{q}$) mesons $B(2\pi^0)/B(4\pi^0) \gtrsim 10$ whereas for X(1810) this ratio is less than a fifth (2) The X(1810) meson appears in the central production reaction

TABLE XI (continued)

X (1750) [65]	0^{++} (2^{++} is less probable)	1755±8	<50	The following decay was observed X (1750) → ηη $\frac{B(X\to\pi^0\pi^0)}{B(X\to\eta\eta)}<0{,}3$	The measurements were performed for P_{π^-} = 38 GeV/c in the region 0,2< |t'|<1 (GeV/c)^2: $d\sigma/d\|t'\|\sim e^{bt'}$, b = 3,8±1,5 (GeV/c)$^{-2}$, $\sigma(\pi^-p\to X(1750)n)\,B(X\to\eta\eta)$ = 3,5±1,5 nb	Exotic meson? (Small width; anomalously low ratio $B(\pi^0\pi^0)/B(\eta\eta)$ for ($q\bar{q}$) mesons
X (1920) [66]	0^{++}, or 1^{-+}, or 2^{++}	1917±15	90^{+35}_{-50}	The following decay was observed X → ηη′: $\frac{B(X\to\eta\eta)}{B(X\to\eta\eta')}<\frac{1}{10}$, $\frac{B(X\to\pi^0\pi^0)}{B(X\to\eta\eta')}<\frac{1}{10}$, $\frac{B(X\to K^0_sK^0_s)}{B(X\to\eta\eta)}<\frac{1}{15}$ (comparison with MIS ITEP)	The measurements were performed for P_{π^-} = 38 GeV/c in the region 0,1 <|t'|<0,6 (GeV/c)^2: $d\sigma/d\|t'\|\sim e^{bt'}$ b = 2±1 (GeV/c)$^{-2}$, $\sigma(\pi^-p\to Xn)\,(X\to\eta\eta')$ =15±5 nb	Glueball with $J^{PC}=0^{++}$; 2^{++}?, hybrid four-quark meson with exotic set of quantum numbers $J^{PC}=1^{-+}$?. (Anomalous ratio B for ordinary ($q\bar{q}$) mesons)
X (2220) [67]	2^{++}	2220±10	<70	The following decay was observed: X → ηη′	$\sigma(\pi^-p\to Xn)\,B(X\to\eta\eta')$ =50±17 nb (38 GeV/c), = 9±3 nb (100 GeV/c)	Apparently the ξ(2220) meson observed in $J/\varphi\to\gamma K\bar{K}$ decays. LASS experiments indicate that this state can be interpreted as the ($s\bar{s}$) meson with $J^{PC}=4^{++}$
X (1640) X (1960) [68]	2^{++} 2^{++}	1643±7 1956±20	<70 220±60	The following decays were observed: X → ωω Ditto	Measurements were performed for p_π = 35 GeV/c in the following reaction: $\pi^-p\to\omega\omega n\to(\pi^0\gamma)(\pi^0\gamma)n$, $\sigma(\pi^-p\to X(1640)n)\times B(X(1640)\to\omega\omega)$ =0,65±0,15 μb, $\sigma(\pi^-p\to X(1960)n)\times B(X(1960)\to\omega\omega)$ =1,0±0,2 μb. Pion exchange predominates in the reactions	The possible interpretation of these states is: radial excitations of the $f_2(1270)$ meson

8. THE G(1590) AND X(1810) MESONS AND OTHER RESULTS OBTAINED BY THE GAMS COLLABORATION

The GAMS collaboration (IHEP, IISN, LAPP, joint IHEP/CERN experiment) has obtained a number of important results in exotic-meson physics. The experiments were performed in parallel on two systems, namely, GAMS-2000, using the pion beam of the IHEP accelerator with momentum $p_\pi = 38$ GeV, and GAMS-4000, using the negative-pion beam of the SPS accelerator at CERN with $p_{\pi^-} = 100$ and 300 GeV/c. Each of these installations incorporated a multichannel hodoscope γ-spectrometer with lead glass counters and a number of additional detectors. The experiments identified the neutral meson decays $M^0 \to \pi^0\pi^0$, $\eta\eta$, $\eta\eta' \to k\gamma$ and so on $k \leqslant 8$–10.

The GAMS experiments were concerned with the production of neutral mesons M_0 in the charge-transfer and central-production reactions discussed above (see Sec. 5.3). The charge-transfer reactions were investigated for $p_{\pi^-} = 38$ and 100 GeV/c:

$$\pi^- p \to M^0 n, \quad \to P_1P_2 \equiv \pi^0\pi^0,\ \eta\eta,\ \eta\eta',\ \eta\pi^0,\ \eta'\pi^0, \quad \to 4\pi^0. \tag{49}$$

Mesons in the final state were identified by determining the effective-mass spectrum of P_1P_2 and $4\pi^0$ states. A partial-wave analysis of the reactions was carried out, and the angular distributions of particles originating in these decays, and enriching the final states with systems having particular sets of quantum numbers, were examined. States formed for transferred momenta $|t'| \sim 0.3$–0.4 (GeV/c)^2 were selected in some cases in order to suppress the background due to peripheral processes.[5)]

For the selected states enriched with the glueball component, an analysis was made of central-production processes at high energies at which a significant contribution due to gluon-gluon collisions was expected (cf. Sec. 5.3.2). These experiments were carried out at $p_{\pi^-} = 300$ GeV/c:

$$\pi^- p \to \pi^-_f\,(M^0 \to \eta\eta,\ 4\pi^0)\,p_s. \tag{50}$$

The GAMS experimental data on the detection and analysis of new exotic mesons are listed in Table XI and are illustrated in Figs. 18–22.

We now turn to a brief summary of these investigations.

8.1. G(1590) as a possible scalar glueball

The scalar meson G(1590) found by the GAMS collaboration in the charge-transfer reaction $\pi^- p \to$ G(1590) $\to \eta\eta$, $\eta\eta'$, $4\pi^0$ at momenta of 38 and 100 GeV/c (Refs. 22, and 62) is very probably a glueball.[21,69] The basis for this interpretation is as follows.

(1) The G(1590) $\to \eta\eta$, $\eta\eta'$, 4π decay probabilities and the upper limits for the decay of this particle along the $K\bar{K}$, $\pi^0\pi^0$ channels are in good agreement with the predictions based on gluon decoloration that is typical of glueball decays and cannot be explained for particles of the usual ($q\bar{q}$) type (cf. Fig. 21).

(2) The G(1590) is clearly seen in the central-production reaction[63] $\pi^- p \to \pi^-_f$ (G(1590) $\to \eta\eta$)p_s at primary momentum of 300 GeV/c at which processes due to the gg interactions of "sea" gluons should be well represented. Actually, while the cross section ratio for the production of G(1590) and the usual ($q\bar{q}$) state, i.e., the f_2(1270) meson, in the charge-transfer reactions (49) is relatively low and amounts to $\sigma(G)/\sigma(f_2) \sim 1/20$, the magnitude of this ratio is greater by an order of magnitude in central-production processes such as (50).

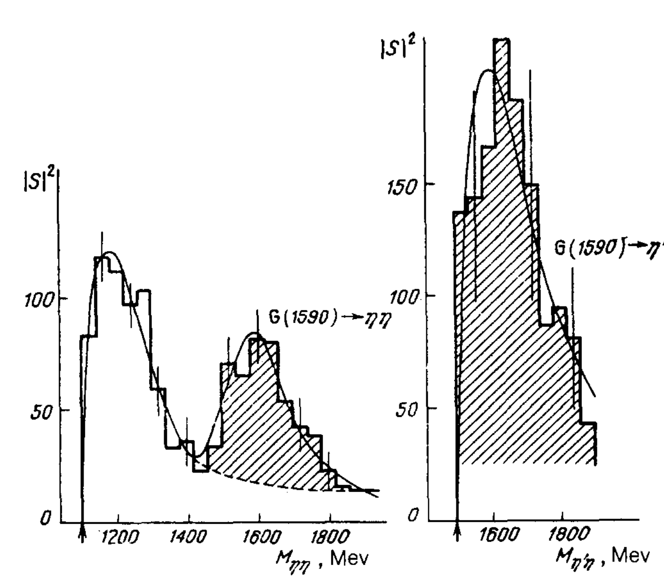

FIG. 18. S-wave intensity in the partial-wave analysis of the $p_\pi = 300$ GeV/c. The region of the G(1590) meson is shown shaded. The curves represent fits by Breit–Wigner resonances with a smooth continuum. The G(1590) meson was discovered in these experiments and its quantum numbers were found to $I^{PC} = 0^{++}$, $I^{PC} = 0^+$.

(3) The mass of G(1590) is not inconsistent with the latest predictions for glueballs based on QCD lattice models, according to which M_0^{++} lies in the range 1240–1600 MeV and $M_{2++}/\mu_{0++} \approx 1.5$.

(4) Searches have been made for the G(1590) meson in the $J/\psi \to \gamma$(gg) channel (12) with enriched gluon component. The MARK III and Crystal Ball experimental data on the $J/\psi \to \gamma\eta\eta$ events is not inconsistent with $J/\psi \to \gamma$G(1590) (see Fig. 23). This problem will require further investigation.

Another possible interpretation of G(1590) as a hybrid or four-quark state was proposed in Ref. 70.

8.2. X(1810) as a tensor glueball

The tensor meson X(1810) was discovered in the charge-transfer reaction $\pi^- p \to$ X(1810)n, X(1810) $\to 4\pi^0$ at momenta of 38 and 100 GeV/c (Ref. 22). Structures with $J^{PC} = 2^{++}$ and 0^{++} in the mass spectrum of the $4\pi^0$ system were distinguished by exploiting the enrichment of events with ϑ_{GJ} when decays of M_0 into two particles were selected according to the symmetrized angle ϑ_{OB} (analogous to the angle ϑ_{GJ} in the Gottfried–Jackson system; see Fig. 19). The exotic character of the X(1810) is indicated by the unusual value of the ratio:

$$B(X(1810) \to 2\pi^0)/B(X(1810) \to 4\pi^0) < 1/5,$$

For the "normal" ($q\bar{q}$) mesons, this ratio lies near ~ 10 (see Sec. 5.2.3). This result, and also the intensive production of X(1810) mesons in the central-production reaction (50), suggests that the glueball interpretation of this hadron is the most likely.

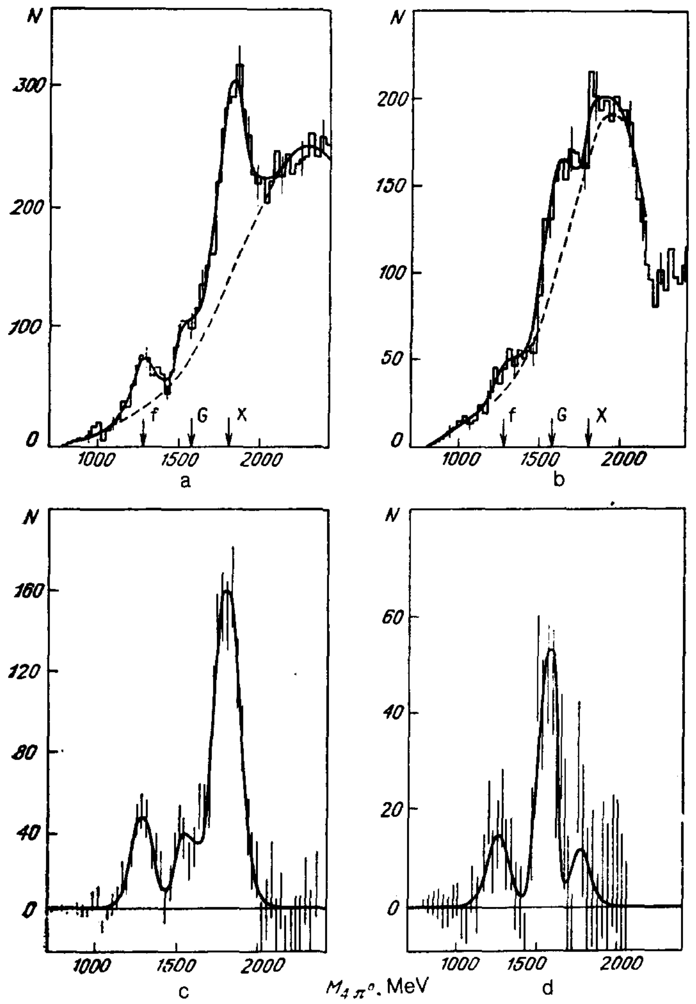

FIG. 19. Studies of the $\pi^- p \to (4\pi^0)n$ reactioon at 100 GeV/c: the invariant-mass spectrum of $4\pi^0$ system. The dominant mechanism in this charge-transfer reaction is pion exchange $[|t'| < 0.15\,\text{GeV}/c)^2]$. a, b—Spectra corresponding to selections in accordance with the cosine of the symmetrized $M \to 4\pi^0$ decay angle $\cos\vartheta_{OB} < 0.4$ ($J^{PC} = 2^+$ selected) and $\cos\vartheta_{OB} > 0.5$ (0^+ selected). The curves represent fits with resonances and a polynomial continuum. c, d—The same mass spectra after the subtraction of the continuum. Arrows show the positions of the resonances F(1270), G(1590), and X(1810).

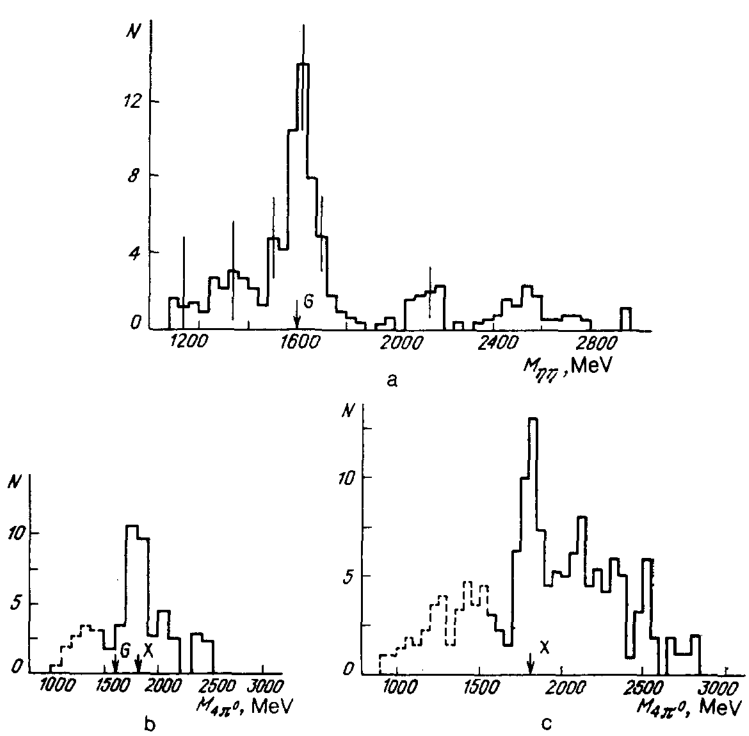

FIG. 20. Central-production reactions for $p_\pi = 300$ GeV/c: a—$\pi^- p \to \pi_f^- (\eta\eta) p_s$, invariant-mass spectrum of the $\eta\eta$ system after the subtraction of the background. The arrow shows the tabulated value of the mass of G(1590). The peak parameters are $M = 1610 \pm 20$ and $\Gamma = 170 \pm 40$ MeV. b—$\pi^- p \to \pi_f^- (4\pi^0) p_s$; $0 < x_f < 0.4$; mass spectrum of the $4\pi^0$ system for the symmetrized $M \to 4\pi^0$ decay angle $\cos\vartheta_{OB} < 0.3$ (2^{++} mesons selected). Peak parameters: $M = 1800 \pm 30$ MeV, $\Gamma = 160 \pm 30$ MeV. Arrows show the masses of X(1810) and G(1590). c—The same reaction for $0.25 < x_F < 0.4$. Because of the absence of the G(1590) signal for lowe x_F, the X(1810) peak is much better defined than in Fig. b.

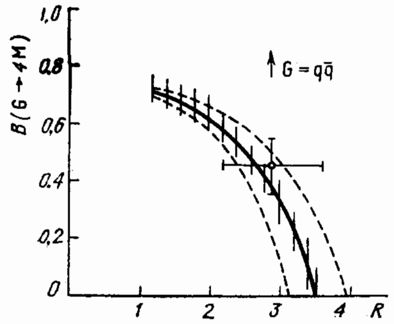

FIG. 21. Calculated decay probability for the process $G(1590)\to 4\pi(B(G\to 4M)$ as a function of the ratio $R = B(G\to\eta\eta)$. The thick curve represents the result for a glueball with $r^2 = B(J/\psi\to\gamma\eta')/B(J/\psi\to\gamma\eta) = 4.7\pm 0.6$ and $\sigma_{\eta\eta}(P_\pi = 38\ \mathrm{GeV}/c = \sigma(\pi^-p\to Gn)B(G\to\eta\eta) = 33\pm 8$ nb (dashed lines show the corridor corresponding to the uncertainty in r^2; vertical bars show the uncertainty in $\sigma_{\eta\eta}$). The open circle represents the experimental result $R = 2.9\pm 0.7$, $B(G\to 4\pi)\approx 5B(G\to 4\pi^0) = 0.46\pm 0.10$. Arrow shows the expected value of $B(G\to 4\pi)$ for $(q\bar{q})$ mesons. The branching ratio B for G(1590) is self-consistent and corresponds to the theoretical description of this meson as a glueball.

8.3. X(1750), X(1920), and other mesons

The GAMS collaboration has also found a number of other mesons that are possible candidates for exotic states of the third kind. Thus, when the charge-transfer reactions $\pi^-p\to\eta\eta n$ and $\pi^-p\to\eta\eta' n$ were investigated from primary momenta of 38 GeV/c in the range $|t'| > 0.2\ (\mathrm{GeV}/c)^2$ (chosen to reduce the background due to peripheral processes), it was found that there were two new narrow states, namely, $X(1750)\to\eta\eta$ and $X(1920)\to\eta\eta'$ (see Fig. 22 and Table XI) that were characterized by anomalous decay probability ratios in the different channels, and were interpreted as possible exotic mesons.

The other mesons listed in Table XI are probably not exotic although their final interpretation is not as yet certain.

Further experiments in this area are in progress at IHEP and CERN, and are planned for BNL.

9. RADIATIVE DECAYS OF J/ψ PARTICLES AND SEARCHES FOR GLUEBALLS

Searches for glueballs have been particularly intensive in studies of the radiative decays $J/\psi\to\gamma(gg)\to\gamma G$ (12), that are expected to have a high probability of production of these exotic states (see Sec. 5.3.1). On the other hand, it is expected that glueballs that do not contain charged valence quarks have small radiative decay widths $\Gamma(G\to\gamma\gamma)$. As already noted in Sec. 5.2.4, these qualitative ideas were used by Chanowitz to formulate the following criterion for glueball identification: $S = (\Gamma(J/\psi\to\gamma G)/\mathrm{LIPS}_1)/\Gamma(X\to\gamma\gamma)/\mathrm{LIPS}_2)\gg 1$ (10).

When the decays (12) were investigated a few years ago, two states were recorded that may well have been glueballs. They were: $\theta(1720)$ with $J^{PC} = 2^{++}$ and, especially, $\iota(1440)$ with $J^{PC} = 0^{-+}$:

$$J/\psi\to\gamma\iota(1440),\quad \iota(1440)\to K\bar{K}\pi\ (J^{PC}=0^{-+}), \tag{51}$$

$$J/\psi\to\gamma\Theta(1720),\quad \Theta(1720)\to K\bar{K},\ \eta\eta,\ \pi\pi\ (J^{PC}=2^{++}) \tag{52}$$

(see Ref. 28 for further details). New information about these states was presented at the Glueballs-88 workshop at BNL.

9.1. ι(1440)

A phase-shift analysis was carried out of data on the decays (51) recorded in MARK III and DM2. These data are in agreement with the quantum numbers of the $\iota(1440)$ meson $J^{PC} = 0^{-+}$, with the mass, $M = 1449\pm 4$ MeV, and the width $\Gamma = 66\pm 7$ MeV (DM2 results). The principal decay channels for this meson are

$$\iota(1440)\to K\bar{K}^*,\ \delta\pi,\quad \delta\to K\bar{K}$$

(50%/50%). The $\iota(1440)\to\rho\gamma$ decay is also a possibility. The high probability of (51) and the relatively low lower limit for the radiative width ($\Gamma(\iota(1440)\to\gamma\gamma)$ can be seen as an argument in favor of the hypothesis that the iota meson is a glueball. It is important to note that the parameter S readily identifies the iota meson among the pseudoscalar mesons: $S_{\pi^0}:S_\eta:S_{\eta'}:S_\iota = 0.02:1:44:(>60-80)$.

9.2. θ(1720)

The Meson $\theta(1720)$, first found in the decay (52), was probably again observed in the $\pi^-p\to K^0_sK^0_sn$ reaction in the MIS spectrometer at IHEP (momentum $p_{\pi^-} = 40$ GeV/c, Ref. 71) and, more clearly, in central collisions observed in

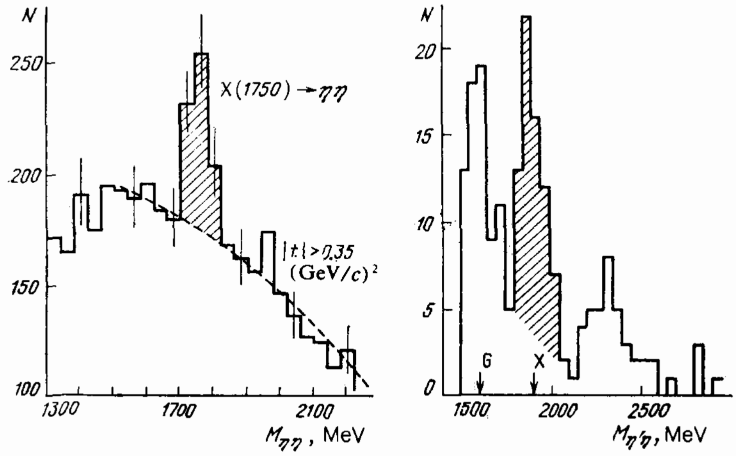

FIG. 22. a—Effective-mass spectrum of the $\eta\eta$ system in the $\pi^-p\to\eta\eta n$ reaction for $|t'| > 0.35\ (\mathrm{GeV}/c)^2$. N is the number of events within the interval $\Delta M = 50$ MeV. b—Invariant-mass spectrum of the $\eta\eta'$ system in the $\pi^-p\to\eta\eta' n$ reaction for $0.2 < |t'| < 0.6\ (\mathrm{GeV}/c)^2$. Arrows show the tabulated masses of G(1590) and X(1920).

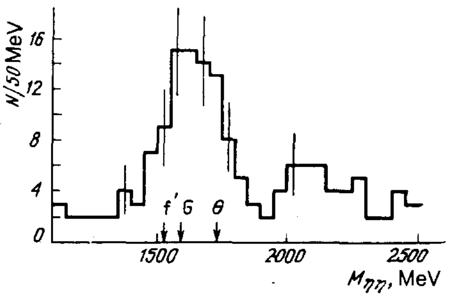

FIG. 23. Resultant effective-mass spectra of the $\eta\eta$ system in $J/\psi \to \gamma\eta\eta$ decays (MARK III, Crystal Ball). Arrows show tabulated masses.

the Ω-spectrometer in the $pp \to p_f(\theta(1720) \to K\bar{K})p_s$ reaction at primary momentum of 300 Gev/c (Ref. 72; cf. Fig. 24). Experiments with colliding e^+e^- beams suggest that $S_\theta > 28$ (Ref. 81).

The $\theta \to KK$ channels are the most common among the $\theta(1720)$ decays. On the other hand, the $\theta(1720)$ meson has not been seen in the $K^-p \to K\bar{K}\Lambda/\Sigma^0$ reaction (LASS, Fig. 24c; MIS IHEP), which is an argument against its interpretation as a meson with the quark structure $s\bar{s}$. We therefore conclude that the available data on the production and decay of $\theta(1720)$ lead to the conclusion that this state may be a glueball. It is important to note in relation to the $\theta(1720)$ meson that the quantum numbers $J^{PC} = 2^{++}$ are the most probable and that $J^{PC} = 0^{++}$ cannot be regarded as finally excluded. Other unanswered questions are those relating to the probability ratios for different decay channels of $\theta(1720)$, if it is interpreted as a glueball.

10. THE E/IOTA PROBLEM

The question that arose following the discovery of the $\iota(1440)$ meson decaying along the $\iota(1440) \to K\bar{K}\pi$ channel in the radiative process (51), was the connetion between this pseudoscalar meson ($J^{PC} = 0^{-+}$) and the state E(1420) that has a similar mass (and decay modes) and has been observed in hadronic processes but, as it turned out, belongs to the axial mesonic nonet ($J^{PC} = 1^{++}$). However, the quantum numbers of the E(1420) meson were not at all reliably determined. The question whether this represents one or more states is referred to as the E/iota problem. It is closely related to experiments on the structure of the axial nonet of mesons, and also the radially-excited pseudoscalar states. To emphasize the differences between the quantum numbers of the E and the iota particles, we shall henceforth speak of pseudoscalar $\iota(1440)/\eta(1440)$ and axial-vector E(1420)/ $f_1(1420)$ mesons (the old designations emphasize the well-established names of these particles and of the E/iota problem itself, whereas the new designations emphasize their quantum numbers).[1] Experimental data on E(1420)/ $f_1(1420)$ and $\iota(1440)/\eta(1440)$ mesons have been obtained

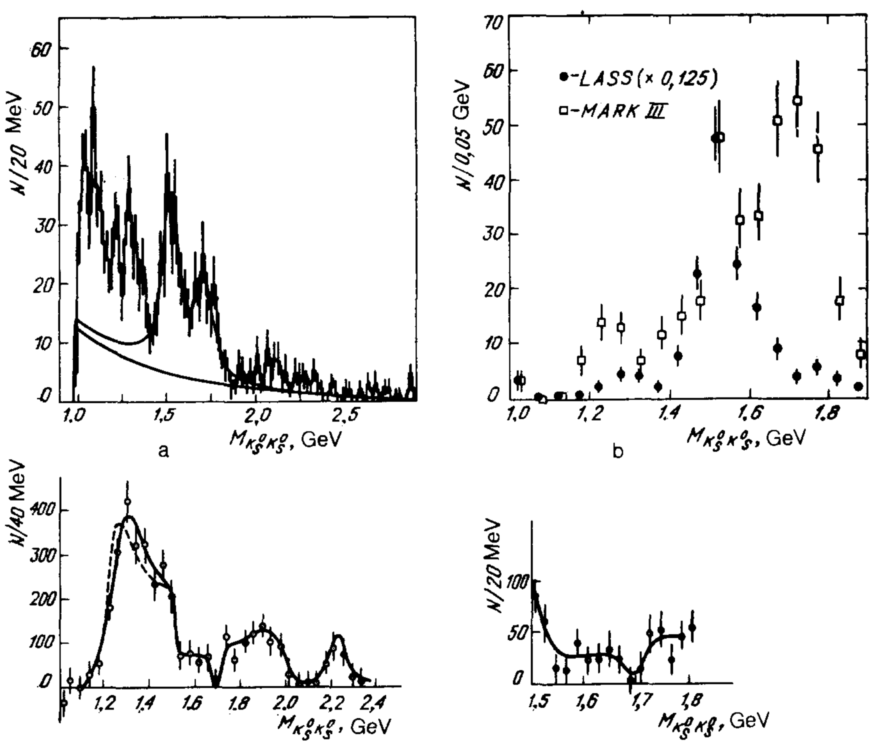

FIG. 24. Data on the $\theta(1720)$ meson, obtained in hadronic processes: a—the $pp \to p_f(K^0_SK^0_S)p_s$ reaction for $p_p = 300$ GeV/c (WA-76); the mass spectrum of $K^0_SK^0_S$ shows a peak with the following parameters: M = 1712 ± 11 MeV and Γ = 138 ± 20 MeV, which are consistent with the $\theta(1720)$ meson. b—Mass spectra of the $K^0_SK^0_S$ system in the $K^-p \to K^0_SK^0_S + \Lambda$(LASS) reaction and in the decays $J/\psi \to \gamma K^0_SK^0_S$(MARK III): $\theta(1720)$ is not produced in K^-p reactions [the data for the two processes were normalized to the yield of S'(1525)]. c—The $\pi^-p \to K^0_SK^0_Sn$ reaction for P_π = 40GeV/c (MIS IHEP): wave intensity $|D_0|^2$ as a function of the $K^0_SK^0_S$ system (left). The mass region of the $\theta(1720)$ meson is shown on the right; a deep minimum, interpreted as diffractive interference of $\theta(1720)$ with F(1270) and f'(1525) can be seen. A rapid variation in the phase difference between the S and D waves occurs in the region of this minimum.

in a number of experiments in which numerous hadronic and electromagnetic processes were investigated. Earlier results and the corresponding bibliographies can be found in the review papers in Refs. 73 and 74. Many new data were presented at the BNL workshop Glueballs-88. The E/iota problem is briefly surveyed below.

10.1. $\bar{p}p$ annihilation reactions

When antiprotons stop in the liquid-hydrogen bubble chamber or a gaseous H_2 target (ASTERIX, new data),[75] they take part in the following reaction:

$$\bar{p}p \to (K_S^0 K^{\pm}\pi^{\mp})\pi^+\pi^-. \quad (53)$$

The inclusive process[76]

$$\bar{p}p \to (K_S^0 K^{\pm}\pi^{\mp})X. \quad (54)$$

has been investigated in experiments with the $\bar{p}$ beam at 6 and 8 Gev/c (recent data are still in the processing state). The $K_s K^{\pm}\pi^{\mp}$ system was studied in reactions (53) and (54), and was found to form a pseudoscalar state ($J^{PC} = 0^{-+}$) with a mass of about 1420 MeV and width of 60–80 MeV. The E(1420)/f_1(1420) meson with $J^{PC} = 1^{++}$ was not seen in these annihilation processes.

10.2. The π^-p charge transfer reactions

The charge-transfer reactions

$$\pi^-p \to (K_S^0 K_S^0 \pi^0)n, \ (K_S^0 K^{\pm}\pi^{\mp})n, \ (\eta\pi\pi)n \quad (55)$$

have been investigated experimentally at BNL and KEK, and very good statistics allowing partial-wave analysis were obtained.[77] The system $K\bar{K}\pi$ was found to have a number of pseudoscalar resonant states with masses of about 1400 and 1460 MeV. The mass spectrum of $\eta\pi\pi$ was found to contain the 0^{-+} resonance with mass of about 1400 MeV. Currently available data on charge-transfer reactions are being interpreted as the production of the ι(1440)/η(1440) meson and the η(1400) meson. The latter is probably the radially excited pseudoscalar state. The production of E(1420)/f_1(1420) mesons has not been observed.

10.3. The K^-p charge-transfer reaction

The charge-transfer reaction

$$K^-p \to (K_S^0 K^{\pm}\pi^{\mp})\Lambda, \quad (56)$$

has been investigated on the LASS installation at 11 GeV/c. Analysis of the ($J^{PC} = 1^{++}$) states did not reveal the presence of the E(1420)/f_1(1420) meson, but the D'(1530)/f_1' (1530) meson was definitely present. These data confirm that it is the D'(1530) and not the E(1420) that is the missing isoscalar member of the axial mesonic nonet.

10.4. Central-production processes

The production of the system $K_s^0 K^{\pm}\pi^{\mp}$ has been investigated in the Ω-spectrometer in the central region of the reaction

$$\pi^-(p) + p \to [\pi^-(p)]_f (K_S^0 K^{\pm}\pi^{\mp}) p_S \quad (57)$$

($p_{\pi^-,p} = 85$ GeV/c, $p_p = 300$ GeV/c; Ref. 79). The effective-mass spectrum was found to contain a well-defined E(1420)/f_1(1420) peak with $J^{PC} = 1^{++}$ (Fig. 25). The

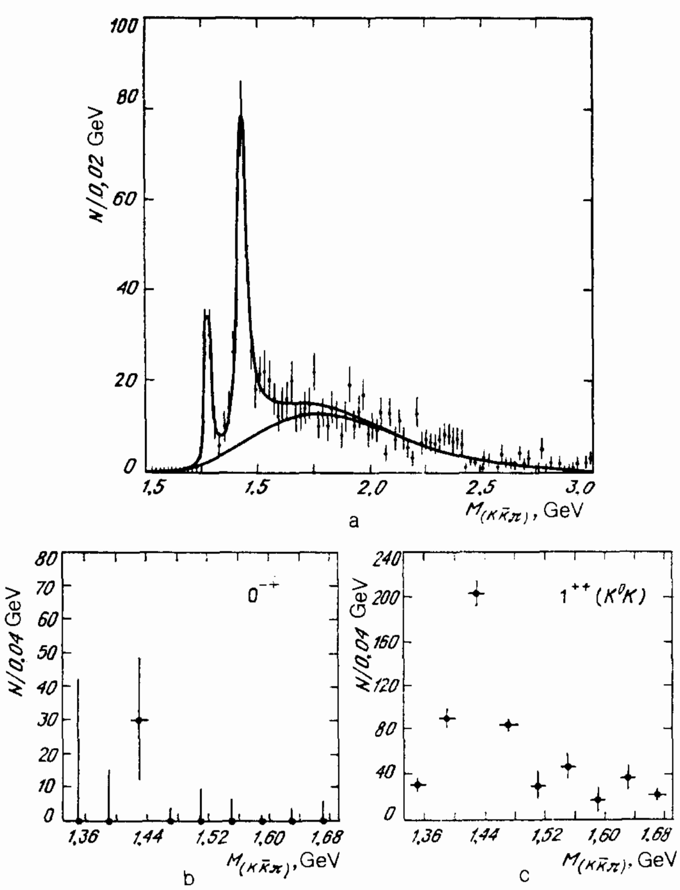

FIG. 25. Production of the E(1420)/f_1(1420) meson in the central region in the $pp \to p_f(K_S^0 K^{\pm}\pi^{\mp})p_s$ reaction. a—Effective-mass spectrum of the $K_S^0 K^{\pm}\pi^{\mp}$ system, b, c—Partial wave analysis for $J^{PC} = 0^{-+}$ and $J^{PC} = 1^{++}$.

possible fraction of the 0^{-+} state does not exceed a few per cent of the 1^{++} state.

10.5. J/ψ decays

Analysis of J/ψ decays in the MARK III and DM2 installations has also produced information on the E/iota problem.

Phase-shift analysis of the system $K\bar{K}\pi$ in $J/\psi\to\gamma K\bar{K}\pi$ radiative decays has revealed that, in addition to the main channel with the pseudoscalar iota meson (51), there was also a contribution due to the 1^{++} state in the region of the $E(1420)/f_1(1420)$ meson.[60]

The $J/\psi\to\omega\ll E$ process was observed in hadronic decays of J/ψ mesons, but $J/\psi\to\varphi\ll E\gg$ was not observed. It follows that "E" cannot be the $s\bar{s}$ system.

The symbol "E" means that this state, with the mass and width of the E(1420) meson, is observed in the effective-mass spectrum of $K\bar{K}\pi$, but its quantum numbers have not been reliably determined.

10.6. $\gamma\gamma^*(Q^2\neq 0)$ collisions

Experiments with colliding e^+e^- beams on the TPC/2γ, MARK II, CELLO, and JADE installations were performed to investigate interactions with "labeled" virtual photons[80,81]:

$$\gamma\gamma^*(Q^2\neq 0)\to K\bar{K}\pi, \qquad (58)$$
$$\to \eta\pi\pi. \qquad (59)$$

Reaction (58) was found to exhibit a very clear $X(1430)\to K\bar{K}\pi$ structure (with the predominance of $K\bar{K}^*$ in the final state). The corresponding data are shown in Fig. 26c. The cross section for this process falls rapidly as $Q^2\to 0$. In accordance with the Landau–Yang theorem, it was concluded from this that the X(1430) state had unit spin. The angular distributions show that the preferred set of quantum numbers of X(1430) is $J^{PC}=1^{++}$, although $J^{PC}=1^{-+}$ cannot be definitely excluded. It is possible that the observed state is the $E(1420)/f_1(1420)$ meson. A peak corresponding to the D(1285) meson (Fig. 26a) is clearly seen in reaction (59). This joint observation of the two mesons in $\gamma\gamma^*$ collisions may be an argument for the conclusions that they belong to the same axial nonet although the values of the corresponding reduced $\gamma\gamma^*$ radiative widths suggest that mixing in this nonet may be very different from the ideal ($\alpha=\vartheta_{A-\vartheta_0}=10-30°$, where θ_0 is the ideal mixing angle). However, before we can arrive at any particular conclusion, we must substantially improve the statistics for (58) and (59), and reliably determine the quantum numbers of the observed resonant states.

This becomes even more important in view of the hypothesis whereby experimental data on the production of the X(1430) in (58) are interpreted as the production of the $\iota(1440)$ meson, based on the analysis of $\iota(1440)\to\gamma\gamma$, $\gamma\gamma^*$ decays and generalized vector dominance.

10.7. Searches for $D(1285)\to\varphi\gamma$ and $E(1420)\to\varphi\gamma$ decays

The rare radiative decay $D(1285)\to\varphi\gamma$ (Fig. 27) was found in Lepton-F experiments. The relative probability and

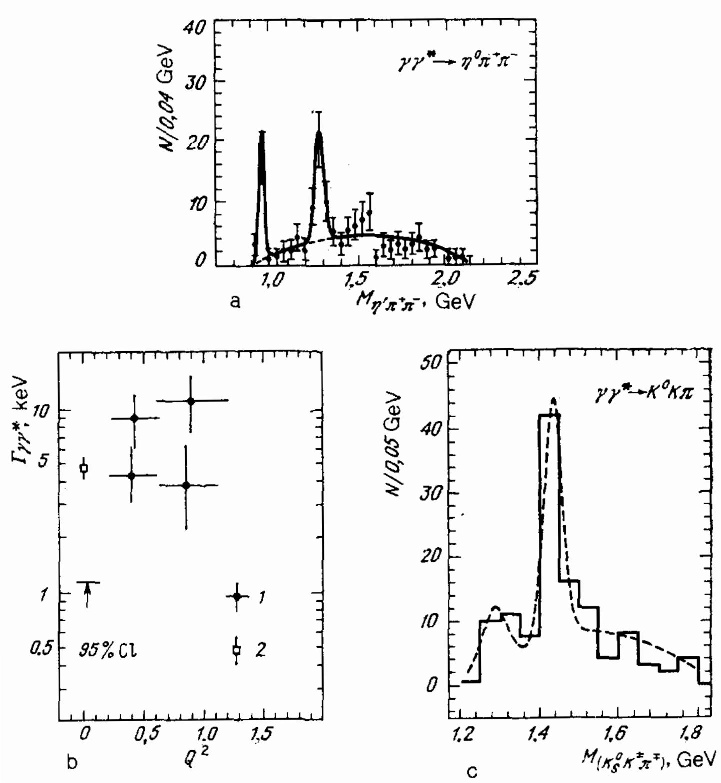

FIG. 26. Experimental data produced by searches for the processes $\gamma\gamma^*(Q^2)\to K^0_S K^\pm\pi^\mp;\eta\pi^+\pi^-$: a—effective-mass spectrum of the $\eta\pi^+\pi^-$ system, obtained with MARK II for events with labelled virtual photons γ^* ($Q^2>0$). This spectrum contains peaks corresponding to the η′(958) and D(1285) mesons. b—Radiative width as a function of Q^2; 1—for the meson with J = 1 (D(1285)), 2—for the meson with J = 0(η′(956)). The figure shows the upper limit (95% confidence level) for D(1285) with $Q^2=0$ [Q^2 is in $(\mathrm{GeV}/c)^2$]. c—Resultant data for the effective-mass spectrum for the $K^0_S K^\pm\pi^\mp$ system obtained on the TPC/2γ, MARK II, CELLO, and JADE systems in $\gamma\gamma^*(Q^2)$ collisions. The summation procedure is not entirely correct because of the different acceptances and different backgrounds. The parameters of the X(1430) peak are: $M=1433\pm 8$ MeV and $\Gamma=42\pm 18$ MeV.

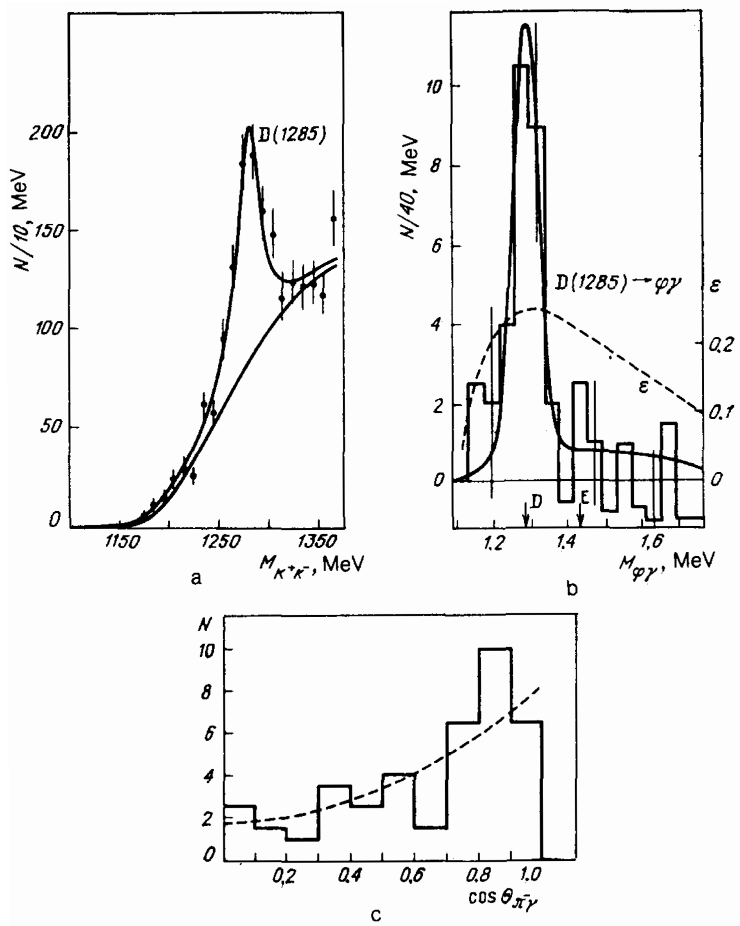

FIG. 27. The D(1285) $\rightarrow \varphi\gamma$ decay recorded in the Lepton-F system: a—effective-mass spectrum of the $K^+K^-\pi^0$ system in the $\pi^-p \rightarrow (K^+K^-\pi^0)n$ reaction. The peak corresponds to the production of the D(1285) meson. The cross section for the $\pi^-p \rightarrow (K^+K^-\pi^0)n$ reaction is about 30 nb ($P_\pi = 32.5$ GeV/c). b—Effective-mass spectrum of the $\varphi\gamma$ system in the $\pi^-p \rightarrow (\varphi\gamma)n$ reaction (after the introduction of the selection criteria for radiative decays). The peak corresponds to the D(1285) $\rightarrow \varphi\gamma$ decay (the width of the peak is determined by instrumental resolution). The arrows show tabulated values of the masses of the D(1285) and E(1420) mesons. The dashed curve and the scale on the right represent the acceptance of the system. c—Angular distribution of $\varphi\gamma$ events from the region of the D(1285) meson ($1230 < M(\varphi\gamma) < 1330$ MeV). This distribution is in good agreement with the quantum numbers $J^P = 1^+$.

the partial width have measured for the process, and the results were[83] $B(D(1285) \rightarrow \varphi\gamma) = (0.9 \pm 0.2 \pm 0.4) \cdot 10^{-3}$ and $\Gamma(D(1285) \rightarrow \varphi\gamma) = 23 \pm 5 \pm 10$ keV. This shows that there is a large $s\bar{s}$ component in the wave funciton of the axial D(1285) meson, i.e., there is a considerable departure from ideal mixing in the axial nonet. On the other hand, the experiments did not reveal the presence of the decay of E(1420), from which it follows, if we use the simple quark model, that E(1420) is unlikely to belong to the axial nonet (cf. also Ref. 84). The Lepton-F experiments are not inconsistent with the interpretation of the E′(1530) as the second isoscalar member of the axial-vector mesonic nonet.

10.8. Resume

The conclusion that we may draw from the above experimental data is that the $\iota(1440)$ meson is probably a glueball, although some of the observed properties of this particle are still unexplained. For example, one relatively puzzling feature is that the iota meson decays along the channel $\iota(1440) \rightarrow \delta\pi$, $\delta \rightarrow K\bar{K}$ (the decay probability is about 50% of all the $K\bar{K}\pi$ decays), while the process $\iota(1440) \rightarrow \delta\pi$, $\delta \rightarrow \eta\pi$, which should occur much more frequently, is not observed. This has been explained by suggesting that the true process is the $\iota(1440) \rightarrow K\bar{K}^* \rightarrow K\bar{K}\pi$ decay and the "δ" signal in the mass spectrum of the $K\bar{K}$ system is simulated by the strong attraction between the kaons in the final state (this is the $K\bar{K}$ molecular model). The remaining open question is: if the $\iota(1440)$ particle is a glueball why is it not formed in central collisons in which G(1590), X(181810), and $\theta(1720)$ mesons, i.e., the other possible glueballs, are clearly seen. It is also not clear whether the pseudoscalar states with masses in the range 1420–1460 GeV, which are seen in $p\bar{p}$ annihilation, πp charge transfer, and J/ψ decay, are in fact the same $\iota(1440)$ meson, or whether they are different particles with similar properties. If the iota meson is produced in all these processes, then this glueball is more highly mixed with the $q\bar{q}$ components than was considered thereto. If this is so, then there is no substantial difference between glueballs and hybrids.

As far as the $E(1420)/f_1(1420)$ meson is concerned, the only process in which this particle has definitely been observed are the central πp and pp collisions in the Ω-spectrometer (if the data on the quantum numbers of mesons in these experiments are the final values, which is subject to

TABLE XII. Some other candidates for the exotic states.

Reference	Processes and particles	Results
1. Refs. 6, 85, and 86	Scalar mesons with $J^{PC}=0^{++}$: $\delta(980)/a_0(980)$, $S^*(975)/f_0(975)$, $\varepsilon(1300)f_0(1300)$. $\chi(1350)/K_0^*(1350)$	Several of the scalar mesons listed in Table III are given the exotic interpretation in which they are regarded as $(q\bar{q})$ mesons (or "extra" states). This interpretation is not generally accepted. (1) $\delta(980)=\frac{1}{\sqrt{2}}(u\bar{u}-d\bar{d})s\bar{s}$, $S^*(975)=\frac{1}{\sqrt{2}}(u\bar{u}+d\bar{d})s\bar{s}$. This model explains the degeneracy in the masses ot these particles and the strong coupling of the S*(975) meson to the $K\bar{K}$ channel. A detailed analysis and a bibliography are given in Ref. 85. (2). $\delta(980)$ and S*(975) have also been treated as $K\bar{K}$ molecules.[86] 3). $\varepsilon(1300)$ and $\varkappa(1350)$ have been interpreted as $(qq\bar{q}\bar{q})$ states.[85]
2. Refs. 87 and 88	Central production of $\pi^+\pi^-$ and K^+K^- states in the reactions $pp\to p_f(\pi^+\pi^-, K^-K^+)p_s$ (ISR), $s^{1/2}=62$ GeV (AFS) (Ref. 87). The $S_1(991)$ meson is a candidate for a glueball	Analysis of $\pi\pi$ and $K\bar{K}$ states has identified scalar mesonic resonances with $J^{PC}=0^{++}$ (Ref. 88): $S_1(991)$ ($g_\pi=0.23, g_K=0.28$), $S_2(998)$ ($g_\pi=0, g_K=0.35$); instead of the S*(975) meson observed earlier in other experiments (g_π, 975 g_K are the coupling constants to $\pi\pi$ and $K\bar{K}$ $\varepsilon(900)$, $\varepsilon(1430)$. Their interpretation is given in Ref. 88 (see also the reviews in Ref. 57 and 74): $\varepsilon(900)\approx\frac{1}{\sqrt{2}}(u\bar{n}+d\bar{d}$, $\varepsilon(1430)$ is the radial excitation of this meson, $S_2(998)\approx s\bar{s}$ and $S_1(991)$ is a candidate for a glueball.
3. Refs. 89 and 90	annihilation of antiprotons stopping in liquid deuterium target $\bar{p}d\to 3\pi^-2\pi^+p_s$ Selection of the process $\bar{p}n\to\pi^-\ \zeta(1480)$, $\to\rho^0\rho^0$. (Ref. 89) in this experiment. Searches for the process $\bar{p}p\to\gamma\zeta(1480)$ (Ref. 90). The state $\zeta(1480)\to\rho^0\rho^0$: $I^G=0^+$ ($I=2$ is unlikely) $J^{PC}=2^{++}$ (maybe 0^{++})	A difference was observed between the inclusive momentum spectra of the negative and positive pions during the annihilation of antiprotons stopping in the liquid-deuterium target. This difference was interpreted as the result of the production of the resonant state $\bar{p}n\to\pi^-X^0$, $X^0\to 2\pi^+2\pi^-$. Analysis of the difference effective-mass spectrum shows that the state X_0 decays along the channel $X^0\to\rho^0\rho^0\to\pi^+\pi^-\pi^+\pi^-$ and had $M=1477\pm 5$ MeV, $\Gamma=116\pm 9$ MeV, $J^{PC}=2^{++}$ (possibly 0^{++}); $I^G=0^+$ ($I=2$ is unlikely). This state is commonly designated $\xi(1480)$. It has been found that $B(\bar{p}n\to\pi^-\zeta)B(\zeta\to 2\rho^0)=11.1\pm 0.8\%$, i.e., $\xi(1380)$ is strongly coupled to the $p\bar{p}$ channel. A possible interpretation is: $\zeta(1480)$ is $(qq\bar{q}\bar{q})$ meson similar to baryonium.[89] Searches have been made for processes involving the production of states such as baryonium in the annihilation of stopping antiprotons $\bar{p}p\to\gamma X^0$ (see, for example, Ref. 90). Monochromatic γ-ray lines corre-ponding to resonant X states have not been found with sufficient statistical precision ($\geqslant 4\delta$). However, several lines have been observed at the 1σ–3σ level. One of them ($E_\gamma=3.559\pm 7.0$ MeV) corresponds to the reaction $\bar{p}p\to\gamma\zeta(1480)$.
4. Ref 91.	Studies of the reaction $\pi^-p\to K_S^0K_S^0n$ for $P_{\pi^-}=40$ GeV/c in the effective-mass range up to 3.6 GeV (MIS IHEP) $X(3075)\to K_S^0K_S^0$ $M=3075\pm 30$ MeV, $\Gamma=170\pm 80$ MeV, $I^G=0^+$, $J^{PC}=4^{++}$	The effective-mass spectrum of the $K_S^0K_S^0$ system is found to contain X(3075) with $M=3075\pm 30$ MeV, $\Gamma=170\pm 80$ MeV, and $I^G=0$, $J^{PC}=4^{++}$ (at the statistical confidence level of $\sim 4\sigma$–5σ). The cross section was found to be $\sigma(\pi^-p\to X(3075)n)B(X(3075)\to K_S^0K_S^0)=10\pm 3\pm 3$ nb. The possible interpretation of this state is that this is an exotic meson or an $s\bar{s}$ state in a deep daughter trajectory,

TABLE XIII. Candidates for crypto-exotic mesons.

	Exotic meson and its decay modes	Quantum numbers	Exotic indicators	Installation
1. Candidates for multiquark mesons and hybrids	C (1480) → $\to \varphi\pi^0$	$I^G = 1^+$, $J^{PC} = 1^{--}$	Anomalously high ratio $R_C = B(C\to\varphi\pi^0)/B(C\to\omega\pi^0) > 0.5$ (95% limit) For the $(q\bar{q})$ mesons it is expected that $R \sim 1/200 - 1/400$. For example, for B(1235), $R_B < 5\cdot 10^{-3}$ (95% limit)	Lepton-F (IHEP)
2. Candidates for glueballs	G (1590) → $\to \eta\eta$, $\eta\eta'$, $4\pi^0$	$I^G = 0^+$, $J^{PC} = 0^{++}$	(1) The ratios of $B(4\pi)$, $B(\eta\eta')$, $BR(\eta\eta)$, $B(\pi\pi)$, $B(K\bar{K})$ are in good agreement with theoretical predictions for a glueball but are anomalous for $(q\bar{q})$ mesons (2) G(1590) is intensively produced in the central region at high energies in gg collisions	GAMS-2000, GAMS-4000 (IHEP-CERN)
	X (1810) → $\to 4\pi^0$	$J^G = 0^+$, $J_{PC} = 2^{++}$	(1). Anomalously high probability of decay along the $X(1810)\to 4\pi^0$ channel: $B(X\to 2\pi^0)/B(X\to 4\pi^0) < 1/5$. (For $(q\bar{q})$ mesons this ratio is greater than 10. (2). X(1810) is intensively produced in the central region at high energies (in gg collisions).	Ditto
	g_T (2010), $g_{T'}$ (2300), $g_{T''}$ (2340) → $\to \varphi\varphi$		Strong departure from the OZI rule is observed in the $\pi^- p\to\varphi\varphi n$ reaction which is saturated by g_T mesons. This may be explained by the contribution of resonances from the intermediate gg channel (i.e., g_T mesons).	
	ι (1440) → $\to K\bar{K}\pi$	$I^G = 0^+$, $J^{PC} = 0^{-+}$	(1) High probability of ι(1440) production in the gluon-enriched decay channel $J/\psi \to \gamma\,(gg) \to \gamma\iota\,(1440)$ (5–10% of the partial width of the $J/\psi\to\gamma$ gg channel). 2) $S_\iota = (\Gamma\,(J/\psi \to \gamma\iota)/LIPS_1 \times (\Gamma\,(\iota \to \gamma\gamma)/LIPS_2)^{-1} > 60-80 \gg 1$	MARK II, «Crystal Ball», MARK III, DM2, CELLO etc.
	θ (1720) → $\to K\bar{K}$, $\pi\pi$, $\eta\eta$	$I^G = 0^+$, $J^{PC} = 2^{++}$ ($J^{PC} = 0^{++}$ is not excluded completely	(1) production of θ(1720) in $J/\psi \to \gamma gg \to \gamma\theta$. 2) $S_\theta > 28 \gg 1$. (3) Production of θ in $p\pi$ and pp collisions in the central region at high energies. (4) θ not produced in $K^- p\to K\bar{K}Y$, i.e., this is not an $s\bar{s}$ meson although there is a strong decay channel $\theta\to K\bar{K}$	MARK II, MARK III, DM2, WA76, MIS—IHEP, LASS
3. Candidates for all types of cryspto-exotic states	X (1750) → $\to \eta\eta$	$I^G = 0^+$, $J^{PC} = 0^{++}$ ($J^{PC} = 2^{++}$, less probable)	(1) Small width $\Gamma < 50$ MeV (2) Anomalous ratio $B\,(\pi^0\pi^0)/B\,(\eta\eta) < 0{,}3$ [for the f(1270) meson, the ratio of the corresponding squares of the matrix elements is approximately 3.4]	GAMS-2000 (IHEP — CERN)
	X (1917) → $\to \eta\eta'$	$I^G = 0^+$, $J^{PC} = 0^{++}$, or 1^{-+}, or 2^{++}	Anomalous BR for the decay channels $B\,(\eta\eta)/B\,(\eta\eta') < 1/10$, $B\,(\pi^0\pi^0)/B\,(\eta\eta') < 1/10$, $B\,(K^0_S K^0_S)/B\,(\eta\eta') < 1/15$	GAMS-2000 (IHEP — CERN)

some doubt because of the simplified procedure used in the analysis based on the distributions on the Dalitz diagram). Studies of the $\gamma\gamma^*(Q^2)$ collisions cannot as yet provide an unambiguous conclusion about the production of the E(1420)/f_1(1420) meson in these processes, although this explanation seems very likely.

If the E(1420)/F_1(1420) meson with quantum numbers 1^{++} does indeed exist, it probably does not belong to the same axial nonet as the D(1285) meson. The second isoscalar member of this nonet, enriched with the $s\bar{s}$ component, is then the D(1520) meson. In that case, the E(1420)/F_1(1420) may be an "extra" exotic hadron. If the $J/\psi \to \omega(K\bar{K}\pi)$ decays do involve the E(1420)/F_1(1420) meson, it may be that this is an argument for its interpretation as a hybrid [cf. (14) in Sec. 5.3.1.].

11. OTHER CANDIDATES FOR EXOTIC MESONS

Table XII lists data on some other contenders for exotic mesons that have been observed in different experiments. The existence and interpretation of these meson is not as yet fully established.

12. BASIC CONCLUSIONS

(1) The last decade has seen considerable successes in searches for exotic hadrons (in the first instance, mesons). Very serious candidates for exotic particles have emerged. Success in this area has largely been due to advances in experimental techniques, nanobarn hadronic spectroscopy, new lines of research such as $J/\psi \to (gg)$; $\gamma\gamma \to R$, and the growing interest in exotic states because of advances in QCD and the emergence of the concept of confinement. Searches for exotic states are closely related to studies of the systematics of ordianry $q\bar{q}$ mesons. Considerable advances have been made in this area in recent years.

(2) There are as yet no reliable candidates for exotic states of the first kind, i.e., states with well-defined exotic properties. There are however, interesting indications of the possible existence of such objects (U mesons and isotensor mesons $X \to VV$).

(3) The $M(1405) \to \eta\pi^0$ meson with $I^G = 1^-$ and $J^{PC} = 1^{-+}$ has been found (GAMS collaboration). It is an exotic state of the second kind (with an exotic set of quantum numbers J^{PC}). It may be the multiquark meson that is the $(qq\bar{q}\bar{q})$ partner of C(1480) with a different charge parity, or the hybrid $g\bar{g}g$. Experiments on the FNAL accelerator, designed to investigate the production of mesons in the Coulomb field of nuclei, suggest that M(1405) should be weakly coupled to the $\rho\pi$ channel $[B(\rho\pi) < 0.03]$.

(4) Most new states that are potential exotic mesons are exotic states of the third kind, i.e., cryptoexotic states. Currently available data on these particles are listed in Table XIII.

(5) It has been suggested that certain other mesonic states are of exotic origin. However, in such cases, either the hypothesis of exotic origin is not properly justified or the state itself is not reliably established ($\delta/a_0(980)$, $S^*/f_0(975)$, $\zeta(1480) \to \rho^0\rho^0$, $X(3075) \to K_s^0 K_s^0$ etc.; cf. Table XII).

(6) The meson $\xi(2210) \to K\bar{K}$, $\eta\eta'$, which was first seen in the decay

$$J/\psi \to \gamma(gg) \to \gamma\xi(2210) \text{ (MARK III)}, \quad \xi(2210) \to K\bar{K}$$

and then in the charge-transfer reactions $\pi^- p \to K_s^0 K_s^0 n$ (MIS IHEP) and $\pi^- p \to \eta\eta' n$ (GAMS-2000), and also in the latest LASS experiments in the $K^- p \to K^+ K^- \Lambda/\Sigma^0$ reaction, was identified as the $(s\bar{s})$ state with $J^{PC} = 4^{++}$ (Ref. 92; cf. Table III).

(7) The E/iota problem and the question of the origin of the E(1420) meson have not as yet been finally settled despite the fact that these studies have been continuing since 1980. The basic results in this area may be summarized as follows:

(a) the E(1420)/f_1(1420) meson with $J^{PC} = 1^{++}$ was observed in central-production processes of the form $\pi^-(p)p \to [\pi^-(p)]_f [K\bar{K}\pi]p_s$ and, possibly, in $\gamma\gamma^*(Q^2) \to K\bar{K}\pi$

(b) the only states observed in the $\pi^- p$ charge transfer and $\bar{p}p$-annihilation reactions were those with $J^{PC} = 0^{-+}$ and, possibly, something else

(c) the $K^- p \to K\bar{K}\pi Y$ reaction examined in the LASS installation revealed the presence of the D′(1530) meson with $J^{PC} = 1^{++}$, but the E(1420) meson was not observed

(d) the radiative decay $D(1285) \to \varphi\gamma$ was found in the Lepton-F installation, but the $E(1420) \to \varphi\gamma$ decay was not.

The conclusion that may be drawn from all these data is that the E(1420)/f_1(1420) meson with $J^{PC} = 1^{++}$ apparently exists, but is unlikely to belong to the same axial nonet as the D(1285) meson, and is an exotic state. The D′(1530) belongs to the axial mesonic nonet.

(8) New independent searches for exotic states are now needed. Research in this area is advancing on a wide front across the world, and includes experiments with hadron beams at IHEP, CERN, BNL, and KEK. Experiments concerned with J/ψ decays are continuing at SPEAR and BEPC, there is a program of research into the annihilation processes on LEAR, and there are many other programs.

I am grateful to L. Montanet for inviting me to present this review to the XXIV Recontre de Moriond under the title "New Results in Hadronic Interactions," which was held on 12–18 March 1989 at Les Arcs, Savoie, France. I am grateful to N. N. Achasov, S. S. Gershteĭn, A. B. Kaĭdalov, V. D. Kekelidze, V. P. Kubarovskiĭ, Yu. D. Prokoshkin, and E. A. Chudakov for a number of useful discussions.

1) In the case of the gg glueballs, the only possibility among the above exotic sets of values of J^{PC} is $J^{PC} = 1^{-+}$; they are all possible for ggg glueballs. It is important to note that the existence of gg glueballs with spin $J = 1$ is doubtful (because of the Landau–Yang theorem that forbids such states for massless gluons).

2) More precisely, a search was made in reaction (3) for charged mesonic resonances with quantum number of $J^P = 1^-$ and $I^G = 1^-$. The set $J^{PC} = 1^{-+}$ characterises neutral mesons belonging to the same isotopic triplets.

3) In this connection, we recall experiments in which a search was made for exotic states $\bar{\rho}(\sim 1600)^+ \to D(1285)\pi^+$ in Coulomb production processes (see Sec. 4.2).

4) Data on J/Ψ decays are reported in Ref. 28 in which a detailed bibliography is also given.

5) Results relating to the discovery by this collaboration of the exotic state of the second kind, namely, the M(1405) meson with $J^{PC} = 1^{-+}$ have already been mentioned (see Sec. 4.1).

[1] G. P. Yost *et al.*, Phys. Lett. B **204**, 1 (1988).

[2]R. L. Jaffe and K. Johnson, *ibid.*, **60**, 201 (1976).
[3]Ya. Ya. lBalitskiĭ *et al.*, Yad. Fiz. **35**, 1300 (1982) [Sov. J. Nucl. Phys. **35**, 761 (1982)].
[4]T. Barnes and F. Close, Phys. Lett. B **116**, 365 (1982).
[5]M. S. Chanowitz, Preprint LBL-16653, Berkeley Ca., 1983; M. S. Chanowitz and S. R. Sharpe, Phys. Lett. B **132**, 413 (1982).
[6]R. L. Jaffe, Phys. Rev. D **15**, 267 and 281 (1977); **17**, 1444 (1978).
[7]R. L. Jaffe and F. E. Low, *ibid.* **17**, 2105 (1979).
[8]E. Witten, Nucl. Phys. **B 156**, 269 (1979).
[9]H. Hogaasen and P. Sorba, *ibid.* **145**, 119 (1978); invited talk at Conference on Hadron Interactions at High Energy, Marseiller, France, June 1978.
[10]M. Bourguin *et al.*, Phys. Lett. B, **172** 113 (1986).
[11]A. N. Aleev *et al.*, Kr. Soobshch. OIYaI No. 19–86, Dubna, 1986, p. 16; Preprints OIYaI, D1-88-368, D1-88-369, Dubna, 1988.
[12]A. Boehnlein *et al.*, Workshop on Glueballs on Hybrids, and Exotic Hadrons, Upton, N. Y., August 29–September 1, 1988, New York, 1989, p. 446.
[13]G. H. N. Shoemaker *et al.*, Phys. Rev. D **37**, 1120 (1988).
[14]N. N. Achasov *et al.*, Z. Phys. C **16**, 55 (1985); **27**, 99; N. N. Achasov, see Ref. 12, p. 509.
[15]B. A. Li and K. F. Liu, Phys. Rev. D **30**, 613 (1984).
[16]J. Olsson, Preprint DESY 87-136, Hamburg, 1987; Kolanoski and P. Zewas, Preprint DESY 87-175, Hamburg, FRG, 1987.
[17]D. Alde *et al.*, Phys. Lett. B **205**, 397 (1988).
[18a)] M. Zielinski *et al.*, Z. Phys. C **31**, 545 (1986).
[18b)] M. Zielinski, Proceedings of the Second International Conference on Hadron Spectroscopy, April 16–18, 1987, Tsukuba, Japan, KEK Report 87-7, 1987, p. 86; see Ref. 12, p. 395.
[19]F. E. Close and H. J. Lipkin, Phys. Rev. Lett. **41**, 1263 (1987).
[20]S. I. Bityukov *et al.*, Yad. Fiz. **38**, 1205 (1983) [Sov. J. Nucl. Phys. **38**, 727 (1983)]; Pis'ma, Zh. Eksp. Teor. Fiz. **42**, 310 (1985) [JETP Lett. **42**, 384 (1985)]; Phys. Lett. B, **188**, 383 (1987); Yad. Fiz. **46**, 506 (1987) [Sov. J. Nucl. Phys. **46**, 273 (1987)], L. G. Landsberg, Preprint IHEP 87-83, Serpukhov, 1987; see also *Proceedings of the International Europhysics Conference on High Energy Physics*, Uppsala, Sweden, June 1987, p. 525.
[21]S. S. Gerstein *et al.*., Z. Phys. C **24**, 305 (1984). S. S. Gerstein, Preprint IHEP 87-42, Serpukhov, 1987.
[22]D. Alde *et al.*, Phys. Lett. B **198**, 286 (1987).
[23]M. S. Chanowitz, *ibid.*, p. 269.
[24]S. Meshkov *et al.*, Invited talk presented at DPF meeting, Salt Lake City, Utah, January 1987.
[25]N. Isgur and J. Paton, Phys. Lett. **B 124**, 247 (1983).
[26]F. E. Close, Preprint RAL-87-072, Chilton, England, 1987.
[27]A. N. Aleev *et al.*, Yad. Fiz. **83**, 1420 (1982) [Sov. J. Nucl. Phys. **36**, 825 (1982)]; Z. Phys. C **25**, 205 (1984); Proceedings of the Quark-86 Seminar at the Institute for Nuclear Research of the USSR Academy of Sciences, Moscow, 1987, p. 255.
[28]L. Kopke and N. Wermes, Phys. Rep. **174**, 67 (1989).
[29]S. S. Gershteĭn and A. A. Logunov, Yad. Fiz. **39**, 1514 (1984) [Sov. J. Nucl. Phys. **39**, 960 (1984)].,
[30]Yu. D. Prokoshkin, Fiz. Elem. Chastits At. Yadra **16**, 584 (1985) [Sov. J.Part. Nucl. **16**, 253 (1985)].
[31]A. Etkin *et al.*, Phys. Lett. B **165**, 217 (1985); **201**, 568 (1988). S. J. Lindenbaum and R. S. Longacre, Int. Conf. on Hadron Spectroscopy, Univ. of Maryland, N. Y., 1985, p. 51.
[32]J. Rosner, Phys. Rev. Lett. **21**, 950, 1468 (1968).
[33]M. Jacob and J. Weyers, Nuovo Cimento B **69**, 521 (1970). V. V. Kishkurno, Elementary Particles, Second School of Physics of the Institute of Theoretical and Experimental Physics [in Russian], Atomizdat, No. 1, 13 (1976); L. G. Landsberg, Preprint IFVE (IHEP) 89-32, Serpukhov, 1989.
[34]J. Allaby *et al.*, Phys. Lett. B **29**, 198 (1969).
[35]D. E. Dorfan *et al.*, Phys. Rev. Lett. **14**, 1003 (1965).
[36]R. M. Bionta *et al.*, *ibid.* **46**, 970 (1981).
[37]H. Burndiers *et al.*, Phys. Lett. B **64**, 107 (1976).
[38]M. S. Alam *et al.*, Phys. Rev. Lett. **40**, 1685 (1978).
[39]S. U. Chung *et al.*, *ibid.* **45**, 1611 (1980).
[40]S. I. Bitukov *et al.*, preprint IFVE (IHEP) 86-242, Serpukhov, 1986.
[41]F. Binon *et al.*, Yad. Fiz. **38**, 934 (1983) [Sov. J. Nucl. Phys. **38**, 561 (1983)]; Nuovo Cimento. B **78**, 313 (1978); Nucl. Methods, Phys. Res. Sect. A, **248**, 86 (1986).
[42]V. P. Kubarovskiĭ, L. G. Landsberg, and V. F. Obraztsov, Yad. Fiz. **48**, 1316 (1988) [Sov. J. Nucl. Phys. **48**, 837 (1988)]; L. G. Landsberg, see Ref. 12, p. 247; Preprint IHEP 88-143, Serpukhov, 1988.
[43]N. N. Achasov, and A. A. Kozhevnikov, Phys. Lett. B **207**, 139 (1988); **209**, 373 (1988).
[44]N. U. Barinov *et al.*, Yad. Fiz. **29**, 1357 (1979) [Sov. J. Nucl. Phys. **29**, 698 (1979)].
[45]N. I. Achasov, Pis'ma Zh. Eksp. Teor. Fiz. **43**, 410 (1986) [JETP Lett. **43**, 526(186)].
[46]F. B. Close and H. J. Lipkin, Phys. Lett. B **196**, 245 (1987).
[47]M. S. Chanowitz, *ibid.* 187, 409.
[48]H. J. Lipkin, see Ref. 18b, p. 363.
[49]J. L. Rosner, *ibid.* p. 395.
[50]F. Close, see Ref. 12, p. 42; S. Godfrey and H. J. Willutzki, *ibid.*, p. 703.
[51]A. B. Clegg, and A. Donnachie, Z. Phys. C **34**, 303 (1987).
[52]Yu. M. Antipov *et al.*, Pis'ma Zh. Eksp. Teor. Fiz. **38**, 356 (1983) [JETP Lett. **38**, 430 (1983)].
[53]M. Atkinson *et al.*, Nucl. Phys. B. **231**, 1 (1984).
[54]M. Atkinson *et al.*, Z. Phys. C **34**, 303 (1987).
[55]R. Longacre, see Ref. 12, p. 625; D. C. Peaslee, *ibid.*, p. 625.
[56]S. L. Lindenbaum, *ibid.* p. 68.
[57] A. Palano, Preprint CERN EP/87-92; Invited Talk at the XXII Rencontre de Moriond, March 1987.
[58]P. S. Booth *et al.*, Nucl. Phys. B **273**, 687 and 689 (1986).
[59]R. Sinha, S. Okuba, and S. F. Tuan, Phys. Rev. D **35**, 952 (1987).
[60]L. Stanco, see Ref. 12, p. 318.
[61]A. M. Badalyan and B. L. Yoffe, Preprint ITEF, No. 3, Moscow, 1986.
[62]F. Binon *et al.*, Nuovo Cimento A **78**, 313 (1983); *ibid.*, **80**, 363 (1984); D. Alde *et al.*, Nucl. Phys. B **269**, 485 (1986).
[63]D. Alde *et al.*, Phys. Lett. B **201**, 160 (1988).
[64]D. Aldi *et al.*, Yad. Fiz. **47**, 1273 (1988) [Sov. J. Nucl. Phys. **47**, 810 (1988)].
[65]D. Alde *et al.*, Phys. Lett. B **182**, 160 (1988).
[66]D. Alde *et al.*, *ibid.* **216**, 447 (1989).
[67]D. Alde *et al.*, *ibid.* **177**, 120 (1986).
[68]D. Alde *et al.*, *ibid.* **216**, 451 (1989).
[69]S. Narison and G. Veneziano, Preprint CERN-TIH 4987/88, Geneva, 1988.
[70]A. N. Achasov and S. F. Gershteĭn, Yad. Fiz. **44**, 1232 (1986) [Sov. J. Nucl. Phys. **44**, 801 (1986)].
[71]O. N. Baloshin *et al.*, *ibid.* **43**, 1487. (1986) [*ibid.* **43**, 959 (1986)] R. V. Bolonkin *et al.*, Nucl. Phys. B **309**, 426 (1988).
[72]T. A. Armstrong *et al.*, see Ref. 12, p. 340.
[73]S. Cooper, Preprint SLAC-PUB-4139, Stanford, 1986.
[74]S. U. Chung, Preprint BNL 40 599-Berkeley, Ca., 1987.
[75]P. Baillon *et al.*, Nuovo Cimento. A **50**, 393 (1987). P. Baillon, Preprint CERN/EP 82-127, Geneva, 1982; Preprint CERN/EP 83.82, Geneva, 1983. S. Ahmad *et al.*, see Ref. 12, p. 246.
[76]D. Reeves *et al.*., Phys. Rev. D **34**, 1950 (1986).
[77]A. Birman *et al.*, Phys. Rev. D **61**, 1557 (1988). M. G. Rath *et al.*, *ibid.*, p. 802. D.Zieminska see Ref. 12, p. 112. A. Ando *et al.*, Phys. Rev. Lett. **57**, 1296 (1986). T. Inagaki, see Ref. 12, p. 356.
[78]D. Aston *et al.*, Phys. Lett. B **201**, 573 (1988).
[79]T. A. Armstrong *et al.*, *ibid.*, **146**, 273 (1988); Z. Phys. C, **34**, 23 (1987).
[80]H. Aihara *et al.*, Phys. Rev. Lett. **57**, 2500 (1986). G. Gidal *et al.*, *ibid.*, **59**, 2012, 2016 (1987).
[81]G. Gidal, Preprint LBL-25532, Berkeley, Ca., 1988; See Ref. 12, p. 171; M. Feindt, *ibid.*, p. 50; Preprint DESY 88-157, Hamburg, 1988.
[82]N. N. Achasov and G. N. Shestakov, Preprint IM SOAN SSSR TF-No. 21 (163), Novosibirsk, 1988.
[83]S. L. Bityukov *et al.*, Phys. Lett. B **203**, 327 (1988). F. I. Bityukov *et al.*, Pis'ma Zh. Eksp. Teor. Fiz. **45**, 368 (1987); [Sov. Phys. JETP **45**, 466 (1988)]; Yad Fiz. **47**, 1258 (1988) [Sov. J. Nucl. Phys. **47**, 800 (1988)].
[84]S. Ishida *et al.*, Preprint Nihon University, NUP A-88-8-Tokyo, 1988.
[85]N. N. Achasov *et al.*, Usp. Fiz. Nauk. **142**, 361 (1984) [Sov. Phys. Usp. **27**, 161 (1984)].
[86]J. Weinstein and N. Isgur, Phys. Rev. Lett. **48**, 659 (1982); Phys. Rev. D **27** 588 (1983).
[87]J. Akesson *et al.*, Nucl. Phys. B **264**, 154 (1986).
[88]K. L. Au *et al.*, Phys. Rev. D **35**, 1653 (1987).
[89]D. Bridges *et al.*, Phys. Rev. Lett. **56**, 211, 215 (1986); **57**, 1534 (1986).
[90]M. Chiba *et al.*, see Ref. 86, p. 117.
[91]O. N. Baloshin *et al.*, Yad. Fiz. **48**, 1213 (1988) [Sov. J. Nucl. Phys. **48**, 770 (1988)].
[92]D. Aston *et al.*, see Ref. 12, p. 160.
[93]G. Kernel, *ibid.*, p. 472.
[94]P. M. Patel, *ibid.*, p. 477.
[95]J. K. Bienlein, *ibid.*, p. 487.
[96]M. T. Ronan, *ibid.*, lp. 494.

Translated by S. Chomet